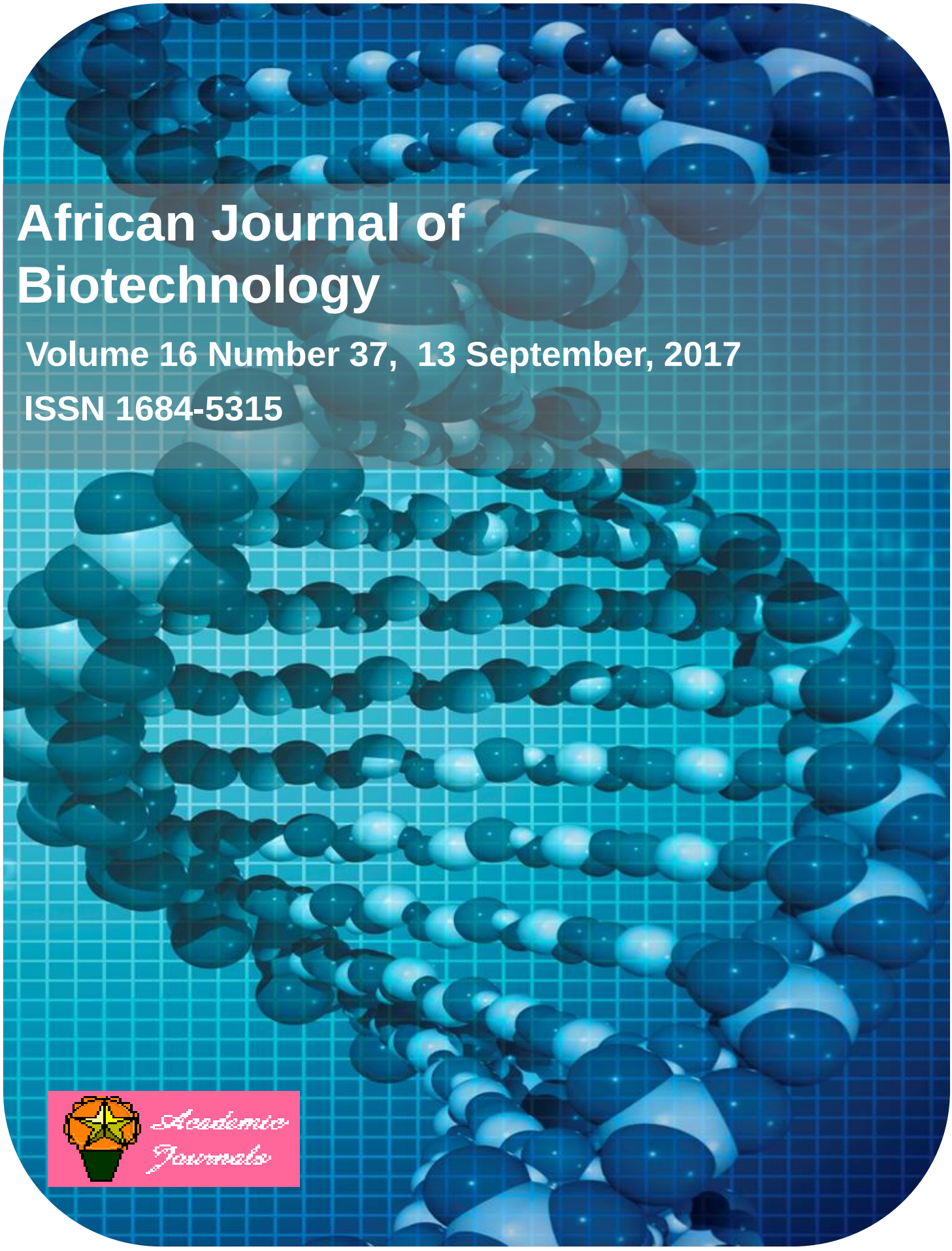

African Journal of Biotechnology

Volume 16 Number 37, 13 September, 2017
ISSN 1684-5315

Academic Journals

ABOUT AJB

The African Journal of Biotechnology (AJB) (ISSN 1684-5315) is published weekly (one volume per year) by Academic Journals.

African Journal of Biotechnology (AJB), a new broad-based journal, is an open access journal that was founded on two key tenets: To publish the most exciting research in all areas of applied biochemistry, industrial microbiology, molecular biology, genomics and proteomics, food and agricultural technologies, and metabolic engineering. Secondly, to provide the most rapid turn-around time possible for reviewing and publishing, and to disseminate the articles freely for teaching and reference purposes. All articles published in AJB are peer-reviewed.

Contact Us

Editorial Office: ajb@academicjournals.org

Help Desk: helpdesk@academicjournals.org

Website: http://www.academicjournals.org/journal/AJB

Submit manuscript online http://ms.academicjournals.me/

Editorial Board

African Journal of Biotechnology

Table of Content: Volume 16 Number 37 13 September, 2017

ARTICLES

academicJournals

Vol. 16(37), pp. 1849-1854, 13 September, 2017
DOI: 10.5897/AJB2017.16150
Article Number: F3A85C865981
ISSN 1684-5315

http://www.academicjournals.org/AJB

African Journal of Biotechnology

Full Length Research Paper

Polymorphism of -308 G/A TNF-α gene correlated with the concentration of TNF-α and lipid profile in obese subject of Javanese population

Pramudji Hastuti*, Demes Chornelia Martantiningtyas, Dewi Karita, Tasmini and Ahmad Hamim Sadewa

Department of Biochemistry, Faculty of Medicine, Universitas Gadjah Mada, Yogyakarta, Indonesia.

Received 13 July, 2017; Accepted 6 September, 2017

Tumor necrosis factor-α (TNF-α) is an adipokine produced in adipocytes which acts as a marker of inflammation. Increased levels of TNF-α have been associated with obesity and abnormal lipid profile. This study aimed to examine the relationship between polymorphism in -308 G/A TNF-α with concentrations of TNF-α, lipid profile and obesity in a Javanese population. The study consisted of 200 participants (98 controls and 102 obese) from a Javanese sample population. All subjects were measured for anthropometry, high-density lipoprotein (HDL)-C, low-density lipoprotein (LDL)-C, triglyceride, cholesterol, and TNF-α levels. Lipid profile were measured using the enzymatic colorimetric method, TNF-α level was measured with enzyme-linked immunosorbent assay (ELISA) and -308 G/A TNF-α polymorphism was detected using Polymerase Chain Reaction-Restriction Fragment Length Polymorphism (PCR-RFLP). Results showed that the GA genotype have LDL-C, triglyceride, cholesterol and TNF-α levels higher than the GG genotype. The findings demonstrate that 308 G/A TNF-α gene polymorphism plays a role in increasing the risk of obesity with odds ratio for A to G allele 1.96 (95% CI = 1.60-2.40) and odds ratio for GA to GG genotype 3.52 (95% CI = 2.84-4.36). TNF-α polymorphism (-308G/A) contributed to increased body mass index and elevated levels of LDL, triglyceride, cholesterol and TNF-α in obese Javanese population. This polymorphism may be used as a marker in the development of metabolic diseases and the identification of risk of obesity. Multifactorial analysis in the future may reveal basic genotypic differences between ethnic groups and demonstrate evidence for other environmental factors.

Key words: Adipokines, lipid profile, obese, polymorphism, populations, tumor necrosis factor-α (TNF-α).

INTRODUCTION

Obesity is a public health problem that has reached epidemic proportions with increasing prevalence worldwide (Rodríguez-Hernández et al., 2013). Obesity is characterized by low-levels of chronic inflammation which play an important role in the pathogenesis of insulin resistance associated with obesity and dyslipidemia (Lee

*Corresponding author: E-mail: pramudji.has@ugm.ac.id. Tel: 62-81578706213.

et al., 2013). In obese people, the liver and tissues exhibit increased activation of kinases such as C-jun of N-terminal kinase and kinase inhibitors, which are able to induce expression of inflammatory cytokines (Stienstra et al., 2012; Solinas and Karin, 2010). These kinases regulate the transcription factor of protein-1 activator, nuclear factor κB, and interferon regulating factor, which induce the regulation of inflammatory mediator gene expression. Increased cytokines aggravate the activation of receptors by positive feedback inhibition of inflammation and inhibitory signaling of metabolic pathways (Boura-Halfon and Zick, 2009). The visceral adipose tissue can produce inflammatory mediators, which induce the production of acute phase reactants, so it is thought that adipose may be an important mediator between obesity and inflammation (Jacobs et al., 2009)

The gene encoding tumor necrosis factor-α (TNF-α) lies in class III of the major histocompatibility complex area on chromosome 6 between human leucocyte antigen-B (HLA-B) and human leucocyte antigen-D related (HLADR) (Zhang et al., 2013). TNF-α binds to two types of outer membrane receptors in target cells, tumor necrosis factor receptor 1 (TNFR1) and TNFR2 which will increase the cellular and pro-inflammatory NF-kB and activation of mitogen-activated protein (MAP) kinase (Locksley et al., 2001).

The function of TNF-α is complex participating in signal transduction pathways and cellular response signal sequences such as apoptosis, proliferation, differentiation, migration, and angiogenesis. Changes in single nucleotides in the promoter region of TNF-α cause the modification of the binding sites of certain transcription factors, and therefore affect the regulation of transcription and modulate their secretion. The A allele of -308G>A TNF-α gene is associated with increased TNF-α expression and is also associated with increased susceptibility and severity of various diseases (Cereda et al., 2012; Chu et al., 2012; Sennikov et al., 2014).

Increased levels of TNF-α were also associated with increased plasma triglyceride (TG), low-density lipoprotein (LDL)-C, low levels of high-density lipoprotein (HD)-C circulation and increased synthesis of fatty acid *de novo* (Zhang et al., 2013). Several studies found there is a relationship between TNF-α-308G/A polymorphism with obesity, metabolic disease and lipid profile (Gupta et al., 2012; Ng et al., 2014), while other studies found no relationship (Romeo et al., 2001; Zhao et al., 2014). The purpose of this study was to investigate the relationship between polymorphism of (-308) G/A TNF-α gene with TNF-α plasma levels and lipid profile in obese Javanese population.

MATERIALS AND METHODS

Subjects

The study consisted of 102 obese subjects with body mass index (BMI>25 kg/m^2) and 98 non obese subjects with BMI 18 to 23 kg/m^2, aged 18 to 35 years. All participants had signed informed consent forms prior to participation and the study was approved by the Medical and Health Research Ethics Committee, Faculty of Medicine, Universitas Gadjah Mada with reference number of KE/FK/532/EC/2016. Subjects were excluded if they were breast-feeding mothers, pregnant women, had infectious diseases, cancer, liver or kidney disease, or taking medications such as anti-hypertension, diabetes, ketosteroid, and hypolipidemic agents.

Anthropometric measurements

Subjects' weight and height were measured and their BMI were calculated. All measurements were measured and double checked by one person to avoid interpersonal variations in measurements.

Measurements of TG, HDL-C, LDL-C, cholesterol and plasma TNF-α concentrations

Five milliliters fasting blood were taken from all subjects and inserted in the EDTA test tube. Blood was centrifuged to get plasma and buffy coat. Plasma is used to measure the lipid profile and TNF-α concentration. Buffy coat were taken for DNA isolation and genotyping. Measurement of TG, HDL-C, and total cholesterol was used with CHOD-PAP method with Diasys kit (Holzheim, Germany). Calculation of LDL was done using the Friedewald formula (Fridewald et al., 1972):

LDL = Total cholesterol - HDL - triacylglycerol / 5

Measurements of plasma TNF-α concentrations were based on the ELISA KIT Human TNF-a Elabscience protocol with detection range of 7.81 to 500 pg/ml.

Genotyping

Genomic DNA was prepared from buffy coat using PROMEGA kit. The G308A polymorphism of TNF-α was shown using primer oligonucleotide (forward primer: 5'-AGG CAA TAG GTT TTG AGGGCC AT-3 'and reverse primer: 5'-TCC TCC CTG CTC CGA TTCCG- 3'). Polymerase chain reaction (PCR) conditions included the initial denaturation at 95°C for 3 min, followed by 35 cycles with temperature of 95°C (1 min), 60°C (1 min), 72°C (1 min), and final extension 72°C (4 min). Product PCR of 107 bp was then cut by 1 U NcoI enzyme restriction and incubated for 3 h at 37°C (87 and 20 bp for -308G and 107 bp for -308A) (Sandhya et al., 2013).

Statistical analysis

Characteristics of subjects, mean of HDL-C, TG, LDL-C, cholesterol, and level of TNF-α between the obese and control groups were tested using unpaired T tests. Comparison of the mean of HDL-C, TG, LDL-C, cholesterol and level of TNF-α plasma between groups of genotypes was done using one-way analysis of variance (ANOVA), followed by the Post-Hoc test. The genotype distribution in each group for each single nucleotide polymorphism (SNP) was tested by the Hardy Weinberg Equilibrium using the Chi-square test. For determination of odd ratio (OR) or relative risk (RR), Chi-square test was used, followed by the Yates' correction test. All statistical analyses were done using SPSS 17 with significant difference of $P < 0.05$.

RESULTS

A total of 200 subjects were involved in this study, with

Table 1. Phenotype, lipid profile and TNF-α plasma level in obese and control groups.

Characteristics		Obese	Control	P
N		102	98	-
Sex	Men	53 (52%)	47 (48%)	-
	Women	49 (48%)	51 (52%)	-
Ages		22.06±4.085	21.14±3.861	0.105
Height (m^2)		1.62±7.98	1.60±7.2	0.030*
Body weight (kg)		82.83±15.17	53.11±8.02	<0.001*
BMI (kg/m^2)		31.05±4.109	20.55±2.185	< 0.001*
HDL-C (mg/dl)		43.16±15.3	58.3±15.38	<0.001*
LDL-C (mg/dl)		116.25±63.14	98.08±55.08	0.032*
TG-C (mg/dl)		155.36±30.48	121.91±21.64	<0.001*
Cholesterol (mg/dl)		163.65±29.19	147.12±39.64	0.001*
TNF- α (pg/ml)		74.94±87.50	44.76±56.00	0.004*

Data is reported in percentage or mean ± SD. *Independent t-test with significance at P<0.05.

Table 2. Comparison of BMI, HDL-C, LDL-C, Triglyceride, Cholesterol and TNF-α level between genotype groups in obese and controls

Variable	Obese (n=102)			Control (n=98)	
	Genotype		P	(GG obese-GA obese)	P
	GG (n=89)	GA (n=13)	(GG obese-GA obese)	GG	GG obese-GG Control)
BMI (kg/m^2)	30.92±4.19	31.88±3.54	0.419	20.55±2.18	<0.001*
HDL-C mg/dl)	44.32±14.77	31.92±14.83	0.003*	58.32±15.38	<0.001*
LDL-C mg/dl)	107.37±51.20	172.07±97.70	<0.001*	98.08±55.08	0.199
Triglyceride (mg/dl)	153.01±30.38	170.14±27.69	0.050	121.91±21.64	<0.001*
Cholesterol (mg/dl)	161.30±26.78	178.42±39.37	0.041*	147.2±39.64	0.006*
TNF-α (pg/ml)	62.86±79.77	151.11±106.24	<0.001*	44.76±56.50	0.049*

*t-test followed by Post-hoc; significantly different if p<0.05.

102 obese subjects with a mean BMI of 31.05 ± 4.109 and 98 non-obese with a mean BMI of 20.55 ± 2.185. As shown in Table 1, there were significant differences for HDL-C, LDL-C, TG, cholesterol, and levels of TNF-α plasma among obese and non-obese groups.

Genotype examination showed that GA carriers were found only in obese subjects and none were found in the controls. Carriers of A allele in this study tend to have higher BMI, LDL-C, TG, cholesterol and plasma TNF-α levels, and lower HDL-C levels when compared with G allele carriers (Table 2).

Comparison of genotype frequencies between control and obese groups was significantly different (P<0.001). In the control group, there were no individual carriers of A. Carriers of A allele were found only in the obese group (11.30%) with an OR of 3.52 (95% CI = 2.84-4.36). Subjects with GA genotype have higher risk for obesity as compared to GG genotype with OR of 1.96 (95% CI = 1.60-2.40) (Table 3).

The distribution of -308 G/A TNF-α genotypes when compared with the Hardy Weinberg equation is as shown in Figure 1 and there were no significant differences (p=0.25).

DISCUSSION

LDL-C, TG, cholesterol and TNF-α plasma in this study were found to be higher in obese subjects as compared to the controls (Table 1). This finding is consistent with the previous research that showed obese individuals to have low HDL levels and high levels of LDL, TG, cholesterol, and TNF-α plasma as compared to the non-obese. These results are similar to previous studies which found abnormal lipid profiles and higher TNF-α levels in obese subjects (Gupta et al., 2012; Ng et al., 2014). In another study, obesity was associated with increased basal lipolysis in adipose tissue and increased free fatty acid, TG and LDL-C in circulation (Souza et al., 2003).

Increased production of TNF-α in adipocytes of obese subjects may contribute to increased basal lipolysis

Table 3. Genotype and allele distribution of TNF-α-308 G/A polymorphism in obese and control groups.

Variable		Obese (n=102, %)	Control (n=98, %)	OR (CI 95%)	P
Genotype	GA	13 (12.7)	0	2.10 (1.81-2.44)	0.0007
	GG	89 (87.3)	98 (100)		
Alelle	A	13 (11.30)	0	2.92 (2.50-342)	0.0000015
	G	102 (88.69)	196 (100)		

*Calculated with chi-square test followed by Yates' correction; significantly different if P<0.05.

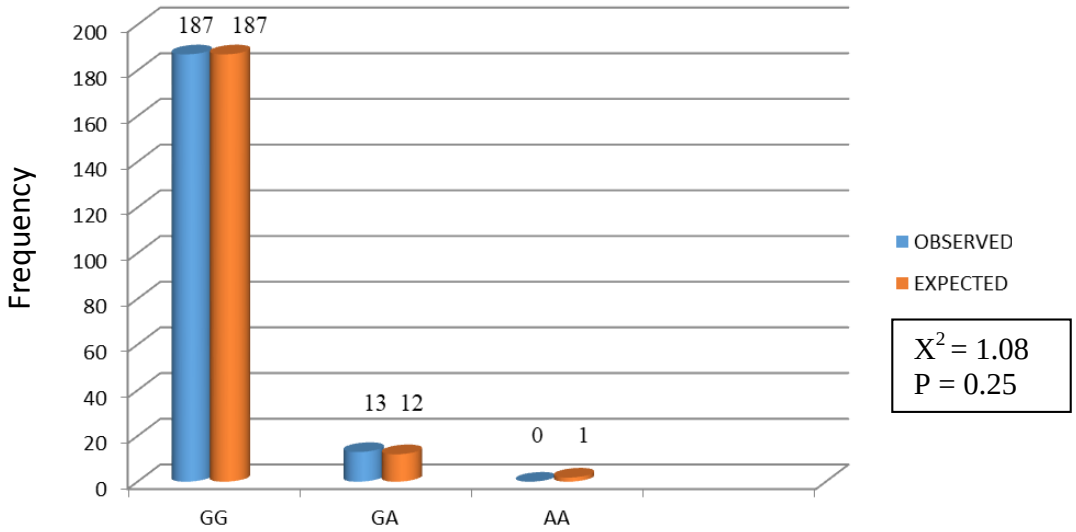

Figure 1. Genotype frequency between observed and expected with Hardy-Weinberg equation.

(Ryden et al., 2002; Ryden et al., 2004). TNF-α gives both autocrine and paracrine signals via TNF-α receptors to activate mitogen-activated protein kinases p44/42 and Januse Kinase (JNK). Active mitogen activated protein kinases p44/42 will affect down regulation of mRNA perilipin (Ryden et al., 2002; Ryden et al., 2004). Another study found that low levels of perilipin are commonly found in obese subjects (Wang et al., 2003).

Increased TNF-α concentration are found in acute and chronic inflammatory conditions, due to the formation of proatherogenic lipid profiles and impaired glucose tolerance. Hyperlipidemia leads to inhibition of acute inflammatory responses. The longer the high TNF-α concentrations found in the circulation, the more they will induce changes in lipid and glucose metabolism. Alteration of lipid induced by TNF-α is proatherogenic (Popa et al., 2007). Patients with inflammatory diseases have lower HDLs and higher ratio of total cholesterol/HDL leading to impaired endothelial function (Boers et al., 2002; Jara et al., 2006). TNF-α modification may also impair cholesterol metabolism. This happens because of the excretion of cholesterol especially as bile acids. Synthesis rate of bile acid in the liver is regulated by the choline-7α-hydroxylase enzyme (CYP7A1) and several cytokines, including TNF-α, which can inhibit the expression and activity of CYP7A1 (De Fabiani et al., 2001). In addition, in human hepatoma cell trials, the activity of sterol 27-hydroxylase and oxysterol 7α-hydroxylase mitochondrial, as rate limiting enzymes in alternative pathways of bile synthesis, is disturbed by TNF-α and other inflammatory cytokines (Memon et al., 2001).

TNF-α (-308) G/A polymorphism in this study was also found to play a role in abnormal lipid profile and high TNF-α plasma concentrations (Table 2). The role of TNF-α (-308) G/A polymorphism is not clearly understood. Nevertheless, this genotype location lies in the sequence consensus for the binding factor of AP-2 transcription in the TNF-α promoter gene region. Research shows the GA genotype in -308 TNF-α polymorphism has higher TNA-α gene expression when compared with GG. Current research has shown that individuals with GA genotypes produce higher TNF-α cytokines (Cereda et al., 2012). Cross-culturally and internationally, the relationship between TNF-α genotype and BMI still varies between regions. This difference may be due to gender

differences, age, ethnic distribution or differences in other confounding factors. For example, the prevalence of allele A carriers appears 45% more frequently in Caucasians, but in Asian populations the frequency is lower (Pyrzak et al., 2010).

In this study, AA genotype of -308G>A TNF-α gene was not found. Frequency of the GA genotype was 12.7% and the GG genotype was 87.3% in the obese group and only the GG genotype in the control group was found. Research on -308G>A TNA-α gene frequency in 3 ethnic populations of Sulawesi, Indonesia (Bugis, Makasar and Toraja) found 2.0% AA genotype, 3.2% GA genotype and 94.8% GG genotype (Lamsis et al., 2002). A-308A TNF-α genotype in some populations varies, for example, in Turkey reaching 40% (Özhan et al., 2010), in Iran 2% (Bonyadi et al., 2014), in Chile 0.6% (Cuenca et al., 2001), India 1% (Sandhya et al., 2013), and in Japan 0% (Ishii et al., 2000).

In this study, A allele of -308 TNF-α gene was found only in obese groups, with higher BMI (31.88 ± 3.54) as compared to G allele (30.92 ± 4.19). The results of this study were in line with those reported by Flores-Ramos et al. (2013), which revealed that the frequency of A allele was found higher in the obese group than non-obese. Our results show the GA genotype was higher as compared to the GG genotype, with RR 2.1 (CI = 1.81-2.44) and A allele was higher than G allele with RR 2.92 (95% CI = 2.50-3.42) as risk factors for obesity. The data of this study provides support for the previous findings that the genetic variants of TNF-α (-308) G/A gene contribute to the development of obesity in some populations (Brand et al., 2001; Hoffstedt et al., 2000).

Research in Polish children found that -308 G/A TNF-α polymorphism is a risk factor for the development of obesity. These results indicate that genetically TNF-α expression plays a role in the development of obesity at young ages, but this effect is influenced by lifestyles of each individual (Pyrzak et al., 2010). Polymorphism of -308 G/A TNF-α gene is associated with several inflammatory diseases as investigated in a Mexican population indicating that gene polymorphism is associated with breast cancer (Flores-Ramos et al., 2013) and chronic obstructive pulmonary diseases in Japan (Sakao et al., 2001) and essential hypertension in the meta-analysis review by Li (2012). Different results were reported in a cohort study in Chinese, Caucasians, and American blacks which found no association between -308 G/A TNF-α polymorphism and obesity (Nieters et al., 2002). Polymorphism of -308 G/A TNF-α was also not associated with Takayasu's arteritis disease in Indian population (Sandhya et al., 2013), acute pancreatitis in Turkish population (Özhan et al., 2010) and inflammatory bowel disease in Iran population (Bonyadi et al., 2014).

Frequency distribution of -308 G/A TNF-α gene in this study when compared with Hardy-Weinberg equilibrium was not significantly different (p= 0.25). This result can be interpreted that the GG, GA and AA genotypes in this study are in accordance with the distribution of genotypes in the population.

Based on the results of this study, it can be concluded that -308 G/A TNF-α polymorphism contributes to increased body mass index, dislipidemia and increased levels of TNF-α in the sample of Javanese obese population. In the future, this polymorphism may be used as a marker in the development of metabolic diseases and the identification of risk of obesity. Multifactorial analysis in the future may reveal basic genotypic differences between ethnic groups and demonstrate evidence for other environmental factors.

CONFLICT OF INTERESTS

The authors have not declared any conflict of interests.

ACKNOWLEDGEMENT

The authors thank Dirjen Dikti of Indonesia for funding the research excellence grant Universitas Gadjah Mada no. 632/UN11-P.III/DIT-LIT/2016.

REFERENCES

Boers M, Dijkmans B, Gabriel S, Maradit-Kremers H, O'Dell J, Pincus T (2004). Making an impact on mortality in rheumatoid arthritis: targeting cardiovascular comorbidity. Arthritis Rheumatol. 50:1734-1739.

Bonyadi M, Abdolmohammadi R, Jahanafrooz Z, Somy MH, Khoshbaten M (2014). TNF-alpha gene polymorphisms in Iranian Azari Turkish patients with inflammatory bowel diseases. Saudi J. Gastroenterol. 20:108-112.

Boura-Halfon S, Zick Y (2009). Phosphorylation of IRS proteins, insulin action, and insulin resistance. Am. J. Physiol. Endocrinol. Metab. 296(4):E581-E591.

Brand E, Schorr U, Kunz I, Kertmen E, Ringel J, Distler A, Sharma AM, (2001). Tumor necrosis factor-alpha–308 G/A polymorphism in obese Caucasians. Int. J. Obes. 25(4):581-585.

Cereda C, Gagliardi S, Cova E, Diamanti L, Ceroni M (2012). The Role of TNF-Alpha in ALS: New hypotheses for future therapeutic approaches. In. Amyotrophic Lateral Sclerosis. InTech. 18:413-436, edited by Martin Maurer http://cdn.intechopen.com/pdfs/26544.pdf

Chu W (2012). Tumor necrosis factor. Cancer Lett. 328(2):222-225.

Cuenca J, Perez CA, Aguierre AJ, Schiattino I, Carlos Aguillon J (2001). Genetic polymorphism at position -308 in the promoter region of the tumor necrosis factor (TNF): Implications of its allelic distribution on susceptibility or resistance to diseases in the Chilean population. Biol. Res. 34(3-4):237-241.

De Fabiani E, Mitro N, Anzulovich AC, Pinelli A, Galli G, Crestani M (2001). The negative effects of bile acids and tumor necrosis factor-α on the transcription of cholesterol 7α-hydroxylase gene (CYP7A1) converge to hepatic nuclear factor-4. J. Biol. Chem. 276:30708-30716.

Flores-Ramos LG, Escoto-De Dios A, Puebla-Pérez AM, Figuera-Villanueva LE, Ramos-Silva A, Ramírez-Patiño R, Delgado-Saucedo JI, Salas-González E, Zúñiga-González GM, Alonzo-Rojo A, .Gutiérrez-Hurtado I, Gallegos-Arreola MP (2013). Association of the tumor necrosis factor-alpha -308G>A polymorphism with breast cancer in Mexican women, Genet. Mol. Res. 12(4):5680-5693.

Friedewald WT, Levy RI, Fredrickson DS (1972). Estimation of the concentration of low-density lipoprotein cholesterol in plasma, without use of the preparative ultracentrifuge. Clin. Chem. 18:499-502.

Gupta V, Gupta A, Jafar T, Gupta V, Agrawal S, Srivastava N, Kumar S, Singh AK, Natu SM, Agarwal CG, Agarwal GG (2012). Association of TNF-α promoter gene G-308A polymorphism with metabolic syndrome, insulin resistance, serum TNF-α and leptin levels in Indian adult women. Cytokine 57(1):32-36.

Hoffstedt J, Eriksson P, Hellstrom L, Rossner S, Ryden M, Arner P, (2000). Excessive fat accumulation is associated with the TNF alpha-308 G/A promoter polymorphism in women but not in men. Diabetologia 43(1):117-120.

Ishii T, Hirose H, Saito I, Nishikai K, Maruyama H, Saruta T (2000). Tumor necrosis factor alpha gene G-308A polymorphism, insulin resistance, and fasting plasma glucose in young, older, and diabetic Japanese men. Metabolism 49(12):1616-1618.

Jacobs M, van Greevenbroek MMJ, van der Kallen CJH, Ferreira I, Blaak EE, Feskens EJM, Jansen EHJ, Schalkwijk CG, Stehouwer CDA (2009). Low-grade inflammation can partly explain the association between the metabolic syndrome and either coronary artery disease or severity of peripheral arterial disease: the CODAM study. Eur. J. Clin. Investig. 39(6):437-444.

Jara LJ, Medina G, Vera-Lastra O, Amigo MC (2006). Accelerated atherosclerosis, immune response and autoimmune rheumatic diseases. Autoimmun Rev. 5:195-201.

Lamsis F, Flannery GR, White NG, Muratore R, Kaelan C, Mitchell RJ (2002). Alleles and haplotypes of tumor necrosis factor (TNF) alpha and beta genes in three ethnic populations of Sulawesi, Indonesia. Hum. Biol. 74(3):381-396,

Lee H, Lee IS, Choue R (2013). Obesity, inflammation and diet. Pediatr Gastroenterol. Hepatol. Nutr. 16:143-152.

Li YY (2012). Tumor necrosis factor-Alpha G308α gene polymorphism and essential hypertension: A Meta-analysis involving 2244 participants. PLoS One 7(4):e35408.

Locksley RM, Killeen N, Lenardo MJ (2001). The TNF and TNF receptor superfamilies: integrating mammalian biology. Cell 104(4):487-501.

Memon RA, Moser AH, Shigenaga JK, Grunfeld C, Feingold KR (2001). In vivo and in vitro regulation of sterol 27-hydroxylase in the liver during the acute phase response. Potential role of hepatocyte nuclear factor-1. J. Biol. Chem. 276:30118-30126.

Ng ZY, Veerapen MK, Hon WM, Lim RLH (2014). Association of leptin/receptor and TNF-α gene variants with adolescent obesity in Malaysia. Pediatr. Int. 56:689-697.

Nieters A, Becker N, Linseisen J (2002). Polymorphisms in candidate obesity genes and their interaction with dietary intake of n-6 polyunsaturated fatty acids affect obesity risk in a sub-sample of the EPIC-Heidelberg cohort. Euro. J. Nutr. 41(5):210-221.

Özhan G, Yanar HT, Ertekin C, Alpertunga B (2010). Clinical study polymorphisms in tumour necrosis factor alpha (TNF) gene in patients with acute pancreatitis. Mediators Inflamm. Article ID 482950, 6 pages.

Popa C, Netea MG, van Riel PLCM, van der Meer JWM, Stalenhoef AFH (2007). The role of TNF-α in chronic inflammatory conditions, intermediary metabolism, and cardiovascular risk. J. Lipid Res. 48:751-762.

Pyrzak B, Wisniewska A, Popko K, Demkow U, Kucharska AM (2010). Association between anthropometric measures of obesity, metabolic disturbances and polymorphism *G*-308A of the tumor necrosis factor-alpha gene in children. Euro. J. Med. Res. 15(Suppl 2):141-146.

Rodríguez-Hernández H, Simental-Mendía LE, Rodríguez-Ramírez G, Reyes-Romero MA (2013). Obesity and inflammation: Epidemiology, risk factors, and markers of inflammation. Int. J. Endocrinol. 11 p, Article ID 678159.

Romeo S, Sentinelli F, Capici F, Arca M, Berni A, Vecci E, Mario UD, Baroni MG (2001). The G-308A variant of the Tumor Necrosis Factor-α (TNF-α) gene is not associated with obesity, insulin resistance and body fat distribution. BMC Med. Genet. 2(1):10-15.

Ryden M, Arvidsson E, Blomqvist L, Perbeck L, Dicker A, Arner P, (2004). Targets for TNF-alpha-induced lipolysis in human adipocytes. Biochem. Biophys. Res. Commun. 318(1):168-175.

Ryden M, Dicker A, van Harmelen V, Hauner H, Brunnberg M, Perbeck L, Lonnqvist F, Arner P (2002). Mapping of early signaling events in tumor necrosis factor alpha-mediated lipolysis in human fat cells. J. Biol. Chem. 277(2):1085-1091.

Sakao S, Tatsumi K, Igari H, Shino Y, Shirasawa H, Kuriyama T (2001). Association of tumor necrosis factor a gene promoter polymorphism with the presence of chronic obstructive pulmonary disease. Am. J. Respir. Crit. Care Med. 163:420-422.

Sandhya P, Danda S, Danda D, Lonarkar S, Luke SS, Sinha S, Joseph G (2013). Tumour necrosis factor (TNF)-α-308 gene polymorphism in Indian patients with Takayasu's arteritis - A pilot study. Indian J. Med. Res. 137:749-752.

Sennikov SV, Vasilyev FF, Lopatnikova JA, Shkaruba NS, Silkov AN (2014). Polymorphisms in the tumor necrosis factor receptor genes affect the expression levels of membrane-bound type I and type II receptors. Mediat. Inflamm. 2014:745909.

Solinas G, Karin M (2010). JNK1 and IKKβ: molecular links between obesity and metabolic dysfunction. FASEB J. 24(8):2596-2611.

Souza SC, Palmer HJ, Kang YH, Yamamoto MT, Muliro KV, Paulson KE, Greenberg AS (2003). TNF-alpha induction of lipolysis is mediated through activation of the extracellular signal related kinase pathway in 3T3-L1 adipocytes. J. Cell Biochem. 89:1077-1086.

Stienstra R, Tack CJ, Kanneganti TD, Joosten LA, Netea MG (2012). The inflammasome puts obesity in the danger zone. Cell Metab. 15:10-18.

Wang Y, Sullivan S, Trujillo M, Lee MJ, Schneider SH, Brolin RE, Kang YH, Werber Y, Greenberg AS, Fried SK (2003). Perilipin expression in human adipose tissues: effects of severe obesity, gender, and depot. Obes. Res. 11(8):930-936.

Zhang BB, Liu XZ, Sun J, Yin YW, Sun QQ (2013). Association between TNF α gene polymorphisms and the risk of duodenal ulcer: a meta-analysis. PLoS One 8(2):e57167.

Zhao Y, Li Z, Zhang L, Zhang Y, Yang Y, Tang Y, Fu P (2014). The TNF-alpha-308G/A polymorphism is associated with type 2 diabetes mellitus: an updated meta-analysis. Mol. Biol. Rep. 41:73-83.

academicJournals

Vol. 16(37), pp. 1855-1862, 13 September, 2017
DOI: 10.5897/AJB2017.16162
Article Number: D7EF9FD65983
ISSN 1684-5315

http://www.academicjournals.org/AJB

African Journal of Biotechnology

Full Length Research Paper

Production of polyhydroxybutyrate (PHB) and biofilm by *Azospirillum brasilense* aiming at the development of liquid inoculants with high performance

Mariana Sanches Santos[1,2], Mariangela Hungria[1,2*] and Marco Antonio Nogueira[1]

[1]Embrapa Soja, C. P. 231, 86001-970, Londrina, Paraná, Brazil.
[2]Department of Biochemistry and Biotechnology, Universidade Estadual de Londrina, C.P. 60001, 86051-990, Londrina, Paraná, Brazil.

Received 22 July, 2017; Accepted 6 September, 2017

Azospirillum brasilense **strains Ab-V5 and Ab-V6 have been broadly and successfully used in commercial inoculants in Brazil, for both non-legumes and legumes, contributing to increases in grain yields with reduced applications of chemical fertilizers.** ***Azospirillum*** **survival, however, may be very low in liquid inoculant formulations and strategies such as the enrichment with polyhydroxybutyrate (PHB) and biofilm may help both bacterial survival and agronomic performance. The production was quantified for both PHB and biofilm by strains Ab-V5 and Ab-V6 in liquid inoculant formulations. Differences were observed between formulations, strains, and strain x formulation. Cellular PHB concentrations ranged from 7.9 to 40.2% of the cell dry weight after 96 h, and considerable amounts of biofilm were synthesized by both Ab-V5 and Ab-V6. Maximum accumulation of PHB and biofilm occurred with** ***A. brasilense*** **strain Ab-V6 in the formulation FORM2+P3, indicating that it is possible to enrich the inoculants on PHB and biofilm by improving the culture media. Field experiments will now be performed to confirm the agronomic efficiency of the improved inoculant.**

Key words: Polyhydroxybutyrate, inoculation, N_2 fixation, plant-growth-promoting bacteria, plant-growth-promoting bacteria (PGPB).

INTRODUCTION

Nitrogen (N) is the nutrient most required for plant growth, and agricultural production and productivity are directly related to its availability to crops. The majority of the Brazilian soils are poor in N, requiring an intense management of chemical N-fertilizers, but the country imports over 70% of the N needed for annual production, resulting in high cost for the farmers (Hungria et al., 2013a). Although N-fertilizers can be easily assimilated by plants, they are also subject to severe losses by leaching and emission into gaseous forms, leading to water pollution, ozone-layer depletion and global warming (Hungria et al., 2013a; Sá et al., 2017). In this context,

*Corresponding author. E-mail: mariangela.hungria@embrapa.br.

the search for alternative biotechnological products, with an emphasis on microbial inoculants, aiming at the total or partial substitution of N-fertilizers, through innovative practices that are environmentally friendly but capable of maintaining high agronomic yields, has been a major goal of investigation (Hungria et al., 2005; Souza et al., 2015; O´Callaghan, 2016; Pereg et al., 2016; Mahanty et al., 2017).

Biological nitrogen fixation (BNF) represents a cheap and sustainable alternative to N-fertilizers and can be promoted by seed inoculation with elite diazotrophic bacteria, contributing to plant's N nutrition (Hungria et al., 2005; Malusá et al., 2012; Ormeño-Orrillo et al., 2013). Although the main contribution of BNF is derived from the symbiosis of bacteria collectively known as rhizobia with legumes, other diazotrophic bacteria less specifically associated with plants, associative or endophytically and contributing to lower amounts of nitrogen can also be important to global saving of N-fertilizers (Bashan and de-Bashan, 2010; Ormeño-Orrillo et al., 2013; Pereg et al., 2016). Furthermore, many of these bacteria have additional mechanisms such as the synthesis of phytohormones, induction of plant-stress tolerance and defense genes, among others (Bashan and de-Bashan, 2010; Fukami et al., 2017a, b), which may help to promote plant growth. Due to their multiple beneficial mechanisms, these bacteria have been classified as plant-growth-promoting bacteria (PGPB), and among them, those belonging to the *Azospirillum brasilense* species are the most studied and employed as inoculants worldwide, with consistent responses to inoculation in all continents, highly contributing to the economy of chemical fertilizers (Okon and Labandera-Gonzalez, 1994; Dobbelaere et al., 2001; Hartmann and Bashan, 2009; Bashan and de-Bashan, 2010; Hungria et al., 2010; Okon et al., 2015; Cassán and Diaz-Zorita, 2016; Pereg et al., 2016; Fukami et al., 2016, 2017a, b).

Liquid inoculants carrying PGPB are easy to handle and can be applied to seeds and by foliar spraying; however, in general, they provide inadequate protection to bacterial cells, leading to early cell death (Stephens and Rask, 2000; Hungria et al., 2005; Tittabutr et al., 2007; Bashan et al., 2014). The improvement of shelf life and maintenance of cell viability can be achieved with the addition of protective molecules such as polymers, which help to maintain water activity and serve as additional supply of carbon and energy to the bacteria (Mugnier and Jung, 1985; Okon and Itzigsohn, 1995; Hungria et al., 2005; Trujillo-Roldán et al., 2013).

Cell viability can also be improved by the synthesis of polyhydroxybutyrate (PHB), a reserve polymer that allows bacteria to withstand environmental stresses (Tal and Okon, 1985; Kadouri et al., 2003; Bhat and Subin, 2015). Kadouri et al. (2003) observed that the synthesis and use of PHB as carbon and energy sources by *A. brasilense* strain Sp7 favored the establishment of this bacterium and its survival in competitive environments under stress conditions. Therefore, it is expected that the accumulation of PHB may favor cell longevity in inoculants. In addition to PHB, biofilm formation provides several benefits to the bacterial community, such as the improvement in bacterial cell-to-cell communication, tolerance of stressful environmental conditions, and host plant colonization (Morris and Monier, 2003; Kreft, 2004; Fukami et al., 2017a). Although studies about the application of biofilms for the benefit of agriculture are scarce, they could contribute to the success of inoculation, protecting bacterial cells from the competition with other soil microbial communities and improving BNF (Jayasinghearachchi and Seneviratne, 2004; Karivaradharajan et al., 2013; Fukami et al., 2017a).

In Brazil, the utilization of *A. brasilense* strains Ab-V5 and Ab-V6 for maize (*Zea mays* L.), wheat (*Triticum aestivum* L.), and brachiarias (*Urochloa* species), as well as for co-inoculation of soybean (*Glycine max* (L.) Merr.) and common bean (*Phaseolus vulgaris* L.) has exponentially grown since 2009 (Hungria et al., 2010, 2013b, 2015, 2016; Hungria, 2011; Marks et al., 2015; Fukami et al., 2016). The objective of this study was to evaluate the production of PHB and biofilm by these two strains of *A. brasilense* in new formulations of liquid inoculants.

MATERIALS AND METHODS

Bacterial strains and growth conditions

The study was performed with *A. brasilense* strains Ab-V5 (=CNPSo 2083) and Ab-V6 (=CNPSo 2084) from the Diazotrophic and Plant Growth-Promoting Bacteria Culture Collection of Embrapa Soja (WFCC #1213, WDCM #1054). Both strains derived from a selection program for cereals (Hungria et al., 2010), and are currently employed for commercial production of *Azospirillum* inoculants in Brazil. The strains were grown in liquid media (FORM2+P3 and FORM4+P6) previously developed in our laboratory (Santos, 2017); the formulations are under registration.

Evaluation of cell dry weight and polyhydroxybutyrate

The strains were single cultured in 500 mL of the liquid formulations (FORM2+P3 and FORM4+P6) for 96 h, at 28±2°C, with agitation of 140 rpm. At 48, 72, and 96 h, 10 mL samples of each treatment were withdrawn and centrifuged at 7,690 *g* for 15 min at 4°C. The supernatant was discarded and the cell mass in the precipitated fraction was washed twice with 5 mL of saline solution (NaCl, 0.85%), followed by further centrifugation, and the supernatant was discarded. The samples were dried at 70°C until constant weight and weighed to determine the cell dry weight (CDW, g L^{-1}) (Belal, 2013). The cells were re-suspended in 12 mL of sodium hypochlorite (NaClO, 5.25%) and incubated for 2 h at 40°C (Karr et al., 1983). The mixture was centrifuged at 2,370 *g* for 15 min at 4°C, and the supernatant discarded. The precipitated fraction was washed successively with 10 mL of distilled water and 96% ethanol (C_2H_6O) (Karr et al., 1983; Hawas et al., 2016). The material was oven dried at 70°C, 1 mL of concentrated sulfuric acid (H_2SO_4) was added, and maintained at 90°C for 30 min, followed by cooling. PHB concentration was obtained by determining the optical density OD_{235}, considering sulfuric acid PA as the blank (Law and

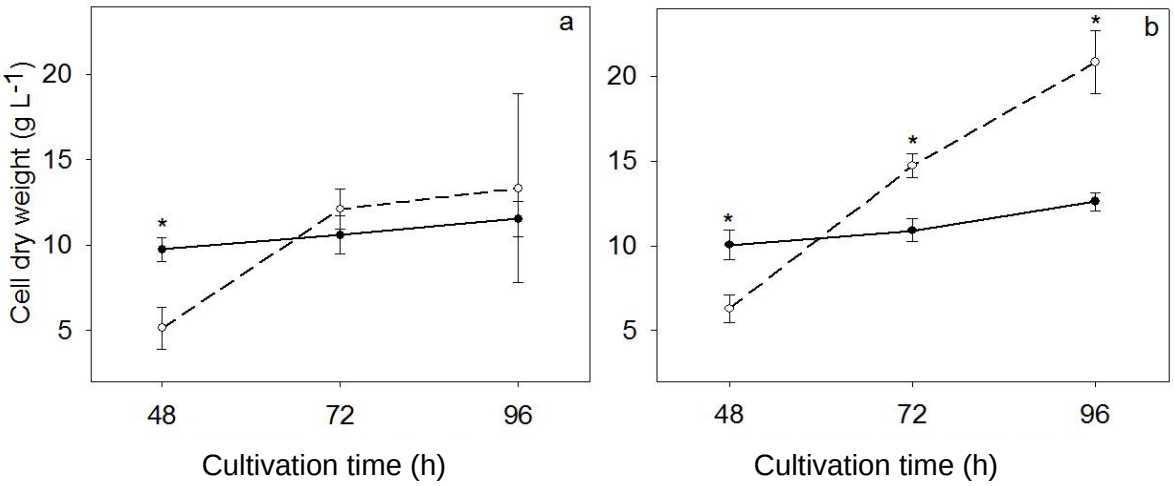

Figure 1. Cell dry weight at 48, 72 and 96 h of cultivation. Solid lines refer to formulation FORM2+P3 and dotted lines refer to FORM4+P6. **(a)** *Azospirillum brasilense* strain Ab-V5. **(b)** *A. brasilense* strain Ab-V6. (*) denotes concentrations that were statistically different by the Tukey test at 5% of probability.

Slepecky, 1960). The amount of PHB present in the sample is provided by the estimate of the crotonic acid ($C_4H_6O_2$) derived from the reaction of the sample with sulfuric acid, using the extinction coefficient of the crotonic acid (1.55×10^4 M^{-1} cm^{-1}). The experiment was performed with three biological replicates, each with three replicates, for each strain and formulation.

From the obtained values of CDW and the absolute PHB concentration of each sample, it was possible to estimate the relative PHB concentration (%), as follows:

$$PHB(\%) = \left(\frac{absolutePHB}{CDW} \right) x100$$

Biofilm formation

Biofilm formation was evaluated after Christensen et al. (1985), with some modifications. The strains were single cultured in 100 mL of the liquid formulations (FORM2+P3 and FORM4+P6) and also in NFb medium (Döbereiner, 1991) for 24 h at 28±2°C, with agitation of 140 rpm. The cultures were then diluted to an OD_{600} of 0.2 and 100 µL of cell suspensions, and transferred to each well of polystyrene microplates with U-bottom (Deltalab S.L.), for each of the three culture media. Plates were incubated in a humid chamber at 28±2°C for 14 days. The culture medium was carefully removed from each well and the plates were dried at 60°C for 1 h, followed by three washes by immersion in 0.9% NaCl and dried at 60°C for 1 h. Next, 100 µL of 0.1% crystal violet ($C_{25}N_3H_{30}Cl$. aqueous solution) were added per well and kept for 20 min. Plates were washed three times by immersion with distilled water. After drying for 1 h at 60°C, 100 µL of 96% ethanol were added to each well and the plates were allowed to stir gently until all the crystal violet was dissolved. Finally, the OD_{570} was determined. The experiment was performed with three biological replicates, each with three replicates, for each strain and formulation.

Statistical analysis

The experimental design was entirely randomized in 2 × 2 factorial, always with three biological replicates, each with three replicates. The data were submitted to the analysis of homogeneity of variance and the means were compared by the Tukey's test ($p \leq 0.05$) using the STATISTICA 7.0 program.

RESULTS

Increases in CDW were observed during the 96 h of growth in both liquid formulations, FORM2+P3 and FORM4+P6, for both strains of *A. brasilense*, Ab-V5 and Ab-V6 (Figure 1). Differences were observed between the strains, being always higher with Ab-V6. Differences were also observed due to the interaction strain × formulation; growth of Ab-V5 was favored by the composition of FORM2+P3, especially in the first 72 h, while for Ab-V6 the CDW at 72 and 96 h was considerably higher in FORM4+6 (Figure 1).

The production of PHB ranged from 2.13 to 5.07 g L^{-1} in FORM2+P3 and from 1.16 to 1.76 g L^{-1} in FORM4+P6, being always higher in the first formulation (Figure 2). Differences between strains were also observed, being always higher in Ab-V6 than in Ab-V5 when grown in FORM2+P3, but with similar and considerably lower accumulation when both strains were grown in FORM4+P6 (Figure 2).

With the CDW values and the PHB concentration, it was possible to estimate the relative PHB concentration (%), which ranged from 7.9 to 40.2% of the CDW (Figure 3). PHB concentration was higher after 96 h of growth for both strains in FORM2+P3. However, in FORM4+P6 the concentration decreased after 48 h, reaching the minimum value after 96 h (Figure 3). Interestingly, although our strains were different in growth capacity, the concentration of PHB was similar for both, but the differences obtained in different media were noticeable, being 4-fold higher for Ab-V6 in FORM2+P3 than in

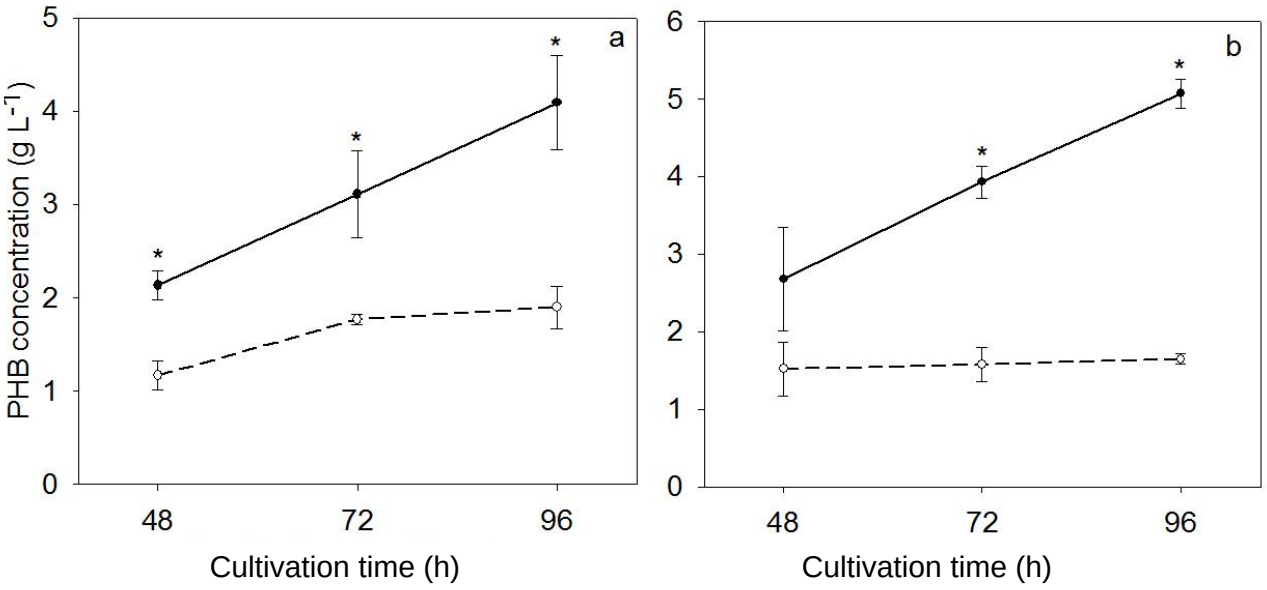

Figure 2. Polyhydroxybutyrate (PHB) concentration at 48, 72 and 96 h of cultivation. Solid lines refer to formulation FORM2+P3 and dotted lines refer to FORM4+P6. **(a)** *Azospirillum brasilense* strain Ab-V5. **(b)** *A. brasilense* strain Ab-V6. (*) Denotes concentrations that were statistically different by the Tukey test at 5% of probability.

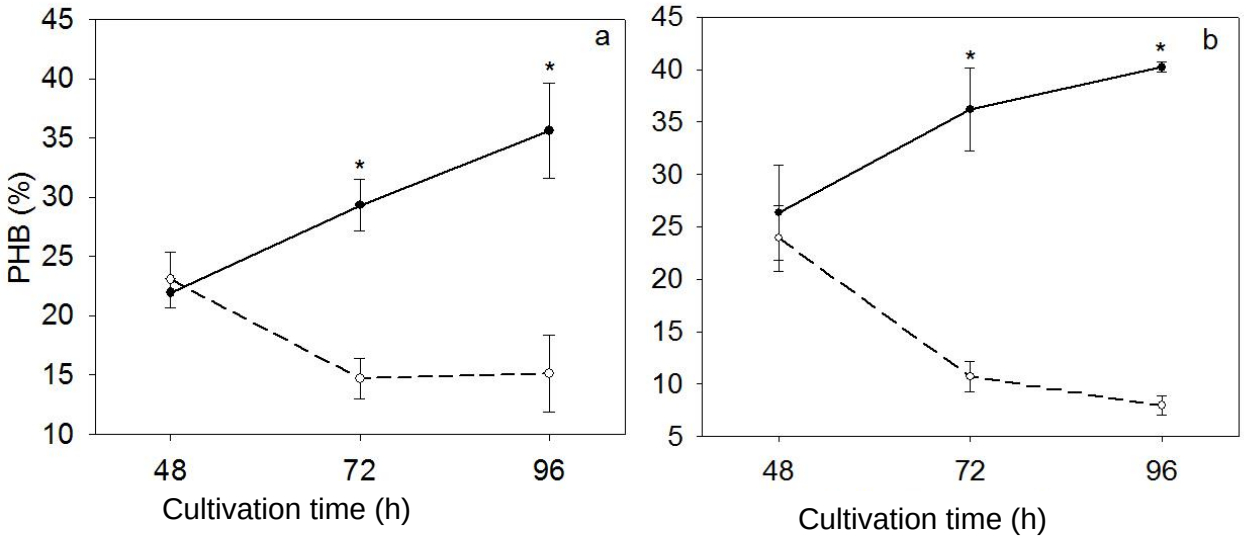

Figure 3. Relative polyhydroxybutyrate (PHB) concentration at 48, 72 and 96 h of cultivation. Solid lines refer to formulation FORM2+P3 and dotted lines refer to FORM4+P6. **(a)** *Azospirillum brasilense* strain Ab-V5. **(b)** *A. brasilense* strain Ab-V6. (*) Denotes concentrations that were statistically different by the Tukey test at 5% of probability.

FORM4+P6 (Figure 3).

Both strains produced similar amounts of biofilm in the formulations FORM2+P3 and FORM4+P6 (Figure 4). *A. brasilense* Ab-V5 synthesized considerable amounts of biofilm in the three culture media, with no differences between them. On the contrary, Ab-V6 strain produced less biofilm in NFb medium and higher in FORM2+P3 and FORM4+P6 (Figure 4).

DISCUSSION

Cell dry weight accumulation and accumulation of polyhydroxybutyrate

Differences in CDW accumulation were observed between *A. brasilense* strains Ab-V5 and Ab-V6, with more growth of Ab-V6, and also as a combined effect of

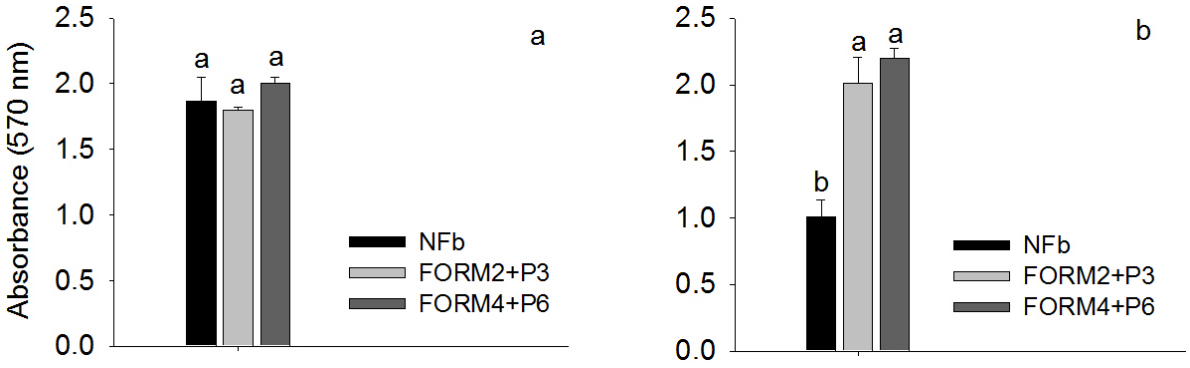

Figure 4. Biofilm formation, evaluated by OD at 570 nm by *Azospirillum brasilense* strains (a) Ab-V5 and (b) Ab-V6 in culture media NFb, FORM2+P3 and FORM4+P6. Letters indicate statistical difference by the Tukey test at 5% probability.

strains × formulation, with more growth of Ab-V5 in FORM2+P3, while the growth of Ab-V6 was favored in FORM4+6. Although the genomes of the two strains show high identity of nucleotides (unpublished genomes, but with average nucleotide identity of 99.99%), differences in the CDW and growth in different formulations point out to probable differences in their metabolism. Other mechanisms controlling cell growth, such as quorum sensing (Boyer and Wisniewski-Dyé, 2009), deserve to be investigated, and indeed, Fukami et al. (2017a) have recently shown differences between Ab-V5 and Ab-V6 in quorum sensing mechanisms.

Differences were also observed between the strains and formulations in the production of PHB, overall being higher in Ab-V6 and in FORM2+P3. Variation in PHB can be attributed both to the composition of the culture medium and to the metabolism of each strain, as suggested by Kamnev et al. (2012). In *Azospirillum*, synthesis of PHB depends on the medium composition and higher PHB values can result in cell flocculation (or aggregation) or in cell changes known as cyst-forms. For example, in a study with *A. brasilense* strain MTCC-125, cell flocculation and higher PHB production (0.13 g L^{-1} of CDW) were observed in medium with cationic compounds (Joe and Sivakumaar, 2009), but the concentration was far lower than in our study with both Ab-V5 and Ab-V6.

PHB concentration (%) represented up to 40.2% of the CDW, being favored by FORM2+P3 with both strains. In *Azospirillum lipoferum* strain Az-204, Vendan and Thangaraju (2007) reported the production of 2.9 mg of PHB per gram of CDW (0.29%) after 96 h of culture in minimal salts medium, considerably lower than with our strains. In contrast, Kamnev et al. (2012) reported that after two days of growth in N-deficient medium and absence of malate, the PHB values obtained with strains Sp7 and Sp245 of *A. brasilense* were 24 and 32% of the CDW, respectively. In another study, Fallik and Okon (1996) reported that PHB in *A. brasilense* ATCC 29729 (Cd) reached 40% of CDW, similar values to those found in our study with strains Ab-V5 and Ab-V6.

Variation in PHB concentration may be related to the consumption of this biopolymer by the cells, as observed by Ratcliff et al. (2008) in the cultivation of *Sinorhizobium meliloti* under nutrient shortage. According to Tal and Okon (1985), the synthesis of PHB is favored under oxygen limitation and by the C:N ratio of the culture medium. In a study by Belal (2013), the best C:N ratio for the PHB production by *Rhizobium etli* E1 and *Pseudomonas stutzeri* E114 was 20:1. A similar ratio resulted in higher production of PHB by *Bacillus cereus* (Belal and Farid, 2016) and by *Pseudomonas boreopolis* J1 (Hawas et al., 2016). This should also explain the results of our study, as for both strains, higher PHB was obtained in FORM2+P3, with C:N ratio 15:1, than in FORM4+P6, with C:N ratio 6:1. In addition, culture media with high C:N ratio can positively influence the aggregation and flocculation of bacterial cells, while low C:N ratio results in more dispersed bacterial growth (Sadasivan and Neyra, 1985; Burdman et al., 1998, 2000), that may improve cell survival and root colonization.

Several beneficial properties of PGPB have been attributed to the synthesis of PHB. It may represent an important carbon and energy source for both cell growth and for the biological nitrogen fixation process in *A. brasilense*, in addition to improve cellular resistance against environmental stresses, such as UV radiation, heat, osmotic pressure, osmotic shock, and desiccation (Tal and Okon, 1985; Kadouri et al., 2003). Flocculation or cyst-forms, also attributed to PHB, is another important property; Joe and Sivakumaar (2009) observed that flocculating cells of *A. brasilense* strain MTCC-125 are rich in PHB and have high tolerance of dissection, while higher PHB accumulation in *A. lipoferum* Az-204 increased the percentage of cysts forms, and consequently, the tolerance of desiccation and high temperature (40°C) (Vendan and Thangaraju, 2007).

Therefore, as indicated by Kadouri et al. (2003), survival of *Azospirillum* in inoculants may be favored by PHB, allowing increased cell viability. In addition, according to the same authors, apparently, the PHB as carbon and energy sources for *A. brasilense* under stress conditions favor the establishment of this bacterium and its survival in competitive environments, although no differences in root colonization were observed (Kadouri et al., 2003). Meanwhile, in field experiments, *A. brasilense* in peat inoculants enriched with PHB (40%) presented better and more consistent results in panicle length and dry weight of maize and foxtail millet (*Setaria italic*) (Fallik and Okon, 1996). Altogether, these reports suggest that the FORM2+P3 would be highly beneficial as inoculant formulation to both Ab-V5 and Ab-V6 strains, favoring the maintenance of cell viability.

Synthesis of biofilm

In this study, an interesting interaction of strain × formulation in the biofilm formation was found; the culture medium did not affect the production by strain Ab-V5, but in Ab-V6, it was significantly lower in the NFb medium. According to Donlan and Costerton (2002), some parameters may influence the biofilm formation, such as nutrient availability, temperature, microbial species and cell number. The composition of the NFb medium, relatively poor in nutrients, and lower in C source than our formulations could explain the lower biofilm production by strain Ab-V6. The results obtained with Ab-V6 corroborate the idea proposed by O'Toole et al. (2000), of continuous production of biofilm by bacteria under non-limited nutrient conditions. Watnick and Kolter (2000) suggested that biofilm-forming microorganisms can return to mobile lifestyles when nutrient availability becomes scarce, a likely response to the search for new sources of nutrients; the change in lifestyle may result in the colonization of new environments (Costerton et al., 1995). However, intriguingly, biofilm formation in Ab-V5 was not affected by the medium composition and as biofilm is also related to quorum sensing (Boyer and Wisniewski-Dyé, 2009; Fukami et al., 2017a), this is an additional evidence pointing out that the differences between the two strains might be related to this mechanism.

In *Azospirillum* spp., biofilm formation is key for root colonization; more specifically, bacteria migrate towards the root by chemotaxis and are attached to the root system, where they proliferate and form micro-colonies, which are fixed to the roots by means of biofilms (Compant et al., 2010; Santi et al., 2013). Noteworthy, Jayasinghearachchi and Seneviratne (2004) observed improvement on N_2 fixation parameters of soybean when a bradyrhizobial-fungal biofilm inoculant (*Bradyrhizobium elkanii* SEMIA 5019 with *Penicillium* species) was used. Therefore, an inoculant enriched in biofilm could benefit plant growth, by improving root colonization by elite PGPB strains.

Conclusion

Inoculants carrying *A. brasilense* strains Ab-V5 and Ab-V6 have been exponentially commercialized in Brazil and other South American countries for both non-legume and legume crops (Hungria et al., 2010, 2013b, 2015, 2016; Hungria, 2011; Marks et al., 2015; Fukami et al., 2016). However, the successful performance of the bacteria relies on their survival under stressing conditions and on an adequate colonization of roots, and PHB accumulation and biofilm formation are keys for the achievement of both processes. Therefore, inoculants enriched with PHB and biofilm are of agronomic interest. In this study, the production of PHB and biofilm by two strains of *A. brasilense* in new formulations of liquid inoculants was evaluated, and the maximum accumulation of PHB and biofilm with *A. brasilense* strain Ab-V6 in the formulation FORM2+P3 was identified. Field experiments will now be performed to confirm the agronomic efficiency of this inoculant.

CONFLICT OF INTERESTS

The authors have not declared any conflict of interests.

ACKNOWLEDGEMENTS

This study was funded by Embrapa (02.13.08.003.00.00), INCT-Plant-Growth Promoting Microorganisms for Agricultural Sustainability and Environmental Responsibility (CNPq-465133/2014-2/ Fundação Araucária/CAPES). The authors acknowledge Dr. Ricardo S. Araujo (Total Biotecnologia) for suggestions on the manuscript. M. S. Santos acknowledges a PhD fellowship from CAPES, M. A. Nogueira and M. Hungria from CNPq.

REFERENCES

Bashan Y, de-Bashan LE (2010). How the plant growth-promoting bacterium *Azospirillum* promotes plant growth- a critical assessment. Adv. Agron. 108:77-136.

Bashan Y, de-Bashan LE, Prabhu SR, Hernandez J (2014). Advances in plant growth-promoting bacterial inoculant technology: Formulations and practical perspectives (1998–2013). Plant Soil 378:1-33.

Belal EB (2013). Production of Poly-hydroxybutyric acid (PHB) by *Rhizobium etli* and *Pseudomonas stutzeri*. Curr. Res. J. Biol. Sci. 5:273-284.

Belal EB, Farid MA (2016). Production of Poly-β-hydroxybutyric acid (PHB) by *Bacillus cereus.* Int. J. Curr. Microbiol. Appl. Sci. 5:442-460.

Bhat SG, Subin RS (2015). Bacterial polyhydroxyalkanoates production and its applications. In. Bhat SG, Nambisan P (eds.), Microbial Bioproducts. Directorate of Public Relation and Publication, Kerala, India. pp. 70-96.

Boyer M, Wisniewski-Dyé F (2009). Cell-cell signalling in bacteria: Not simply a matter of quorum. FEMS Microbiol. Ecol. 70:1-19.

Burdman S, Jurkevitch E, Shwartsburd B, Hampel M, Okon Y (1998). Aggregation in *Azospirillum brasilense*: effects of chemical and physical factors and involvement of extracellular components. Microbiology 144:1989-1999.

Burdman S, Jurkevitch E, Soria-Diaz ME, Serrano AMG, Okon Y (2000). Extracellular polysaccharide composition of *Azospirillum brasilense* and its relation with cell aggregation. FEMS Microbiol. Lett. 189:259-264.

Cassán F, Diaz-Zorita M (2016). *Azospirillum* sp. in current agriculture: From the laboratory to the field. Soil Biol. Biochem. 103:117-130.

Compant S, Cle´Ment C, Sessitsch A (2010). Plant growth-promoting bacteria in the rhizo- and endosphere of plants: their role, colonization, mechanisms involved and prospects for utilization. Soil Biol. Biochem. 42:669-678.

Costerton JW (1995). Overview of microbial biofilms. J. Ind. Microbiol. 15:137-40.

Christensen GD, Simpson WA, Younger JJ, Baddour LM, Barrett FF, Melton DM, Beachey EH (1985). Adherence of coagulase-negative staphylococci to plastic tissue culture plates: A quantitative model for the adherence of staphylococci to medical devices. J. Clin. Microbiol. 22:996-1006.

Dobbelaere S, Croonenborghs A, Thys A, Ptacek D, Vanderleyden J, Dutto P, Labandera-Gonzalez C, Caballero-Mellado J, Aguirre JF, Kapulnik Y, Brener S, Burdman S, Kadouri D, Sarig S, Okon Y (2001). Responses of agronomically important crops to inoculation with *Azospirillum*. Aust. J. Plant Physiol. 28:871-879.

Döbereiner J (1991). The genera *Azospirillum* and *Herbaspirillum*. In. Ballows A, Trüper HG, Dworkin M, Harder W, Shleifer K, (eds.), The Prokaryotes. Springer-Verlag, New York. pp. 2236-2253.

Donlan RM, Costerton JW (2002). Biofilms: Survival mechanisms of clinically relevant microorganisms. Clin. Microbiol. Rev. 15:167-193.

Fallik E, Okon Y (1996). Inoculants of *Azospirillum brasilense*: Biomass production, survival and growth promotion of *Setaria italica* and *Zea mays*. Soil Biol. Biochem. 28:123-126.

Fukami J, Abrantes JLF, del Cerro P, Nogueira MA, Megías M, Ollero FJ, Hungria M (2017a). Revealing different strategies of quorum sensing in *Azospirillum brasilense* strains Ab-V5 and Ab-V6. Arch. Microbiol.

Fukami J, Nogueira MA, Araujo RS, Hungria M (2016) Accessing inoculation methods of maize and wheat with *Azospirillum brasilense.* AMB Express 6(3):1-13.

Fukami J, Ollero FJ, Megías M, Hungria M (2017b). Phytohormones and induction of plant-stress tolerance and defense genes by seed and foliar inoculation with *Azospirillum brasilense* cells and metabolites promote maize growth. AMB Express 7:153.

Hartmann A, Bashan Y (2009). Ecology and application of *Azospirillum* and other plant growth-promoting bacteria (PGPB). Eur. J. Soil Biol. 45:1-2.

Hawas LME, El-Banna TE, Belal EBA, El-Aziz AA (2016). Production of bioplastic from some selected bacterial strains. Int. J. Curr. Microbiol. Appl. Sci. 5:10-22.

Hungria M (2011). Inoculação com *Azospirillum brasilense*: Inovação em Rendimento a Baixo Custo. Documentos, 325, Embrapa Soja, Londrina, Brazil, 37p.

Hungria M, Campo RJ, Souza EM, Pedrosa FO (2010). Inoculation with selected strains of *Azospirillum brasilense* and *A. lipoferum* improves yields of maize and wheat in Brazil. Plant Soil 331:413-425.

Hungria M, Loureiro MF, Mendes IC, Campo RJ, Graham PH (2005). Inoculant preparation, production and application. In. Werner W. Newton WE (eds.), Nitrogen Fixation in Agriculture, Forestry, Ecology and the Environment. Springer, Dordrecht, Amsterdam. Pp. 223-254.

Hungria M, Mendes IC, Mercante FM (2013a). A Fixação Biológica do Nitrogênio como Tecnologia de Baixa Emissão de Carbono: Avaliação nas Culturas do Feijoeiro e da Soja. Documentos, 337, Embrapa Soja, Londrina, Brazil, 22p.

Hungria M, Nogueira MA, Araujo RS (2013b). Co-inoculation of soybeans and common beans with rhizobia and azospirilla: Strategies to improve sustainability. Biol. Fertil. Soils 49(7):791-801.

Hungria M, Nogueira MA, Araujo RS (2015). Soybean seed co-inoculation with *Bradyrhizobium* spp. and *Azospirillum brasilense*: A new biotechnological tool to improve yield and sustainability. Am. J. Plant Sci. 6:811-817.

Hungria M, Nogueira MA, Araujo RS (2016). Inoculation of *Brachiaria* spp. with the plant growth-promoting bacterium *Azospirillum brasilense*: an environment-friendly component in the reclamation of degraded pastures in the tropics. Agric. Ecosyst. Environ. 221:125-131.

Jayasinghearachchi HS, Seneviratne GA (2004). A bradyrhizobial-*Penicillium* spp. biofilm with nitrogenase activity improves N_2 fixing symbiosis of soybean. Biol. Fertil. Soils 40:432-434.

Joe MM, Sivakumaar PK (2009). Role of certain cationic compounds on the enhancement of flocculation in *Azospirillum brasilense* MTCC-125: Bioinoculation effect on growth of sunflower. Die Bodenkultur: J. Land Manag. Food Environ. 60:5-13.

Kadouri D, Jurkevitch E, Okon Y (2003). Involvement of the reserve material poly-β-hydroxybutyrate in *Azospirillum brasilense* stress endurance and root colonization. Appl. Environ. Microbiol. 69:3244-3250.

Kamnev AA, Tugarova AV, Tarantilis PA, Gardiner PHE (2012). Comparing poly-3-hydroxybutytateaccumulation in *Azospirillum brasilense* strains Sp7 and Sp245: The effect of copper (II). Appl. Soil Ecol. 61:213-216.

Karivaradharajan S, Prasanna R, Kumar A, Pattnaik S, Chakravarty K, Shivay YS, Singh R, Saxena AK (2013). Evaluating the influence of novel cyanobacterial biofilmed biofertilizers on soil fertility and plant nutrition in wheat. Eur. J. Soil Biol. 55:107-116.

Karr DB, Waters JK, Emerich DW (1983). Analysis of Poly-,3-Hydroxybutyrate in Rhizobium japonicum Bacteroids by Ion-Exclusion High-Pressure Liquid Chromatography and UV Detection. Appl. Environ. Microbiol. 46:1339-1344.

Kreft JU (2004). Biofilms promote altruism. Microbiology 150:2751-2760.

Law JH, Slepecky RA (1960). Assay of poly-β-hydroxybutyric acid. J. Bacteriol. 82:33-36.

Mahanty T, Bhattacharjee S, Goswami M, Bhattacharyya P das B, Ghosh A, Tribedi P (2017) Biofertilizers: a potential approach for sustainable agricultrue development. Environ. Sci. Pollut. Res. 24:3315-3335.

Malusá E, Sas-Paszt L, Ciesielska J (2012). Technologies for beneficial microorganisms inocula used as biofertilizers. Sci. World J 2012:1-12.

Marks BB, Megías M, Ollero FJ, Nogueira MA, Araujo RS, Hungria M (2015). Maize growth promotion by inoculation with *Azospirillum brasilense* and metabolites of *Rhizobium tropici* enriched on lipo-chitooligosaccharides (LCOs). AMB Express 5:71.

Morris CE, Monier JM (2003). The ecology significance of biofilm formation by plant-associeted bacteria. Annu. Rev. Phytophatol. 41:429-453.

Mugnier J, Jung G (1985). Survival of bacteria and fungi in relation to water activity and the solvent properties of water in biopolymer. Appl. Environ. Microbiol. 50:108-114.

O´Callaghan M (2016). Microbial inoculation of seed for improved crop performance: issues and opportunities. Appl. Microbiol. Biotechnol. 100:5729-5746.

O'Toole G, Kaplan HB, Kolter R (2000). Biofilm formation as microbial development. Annu. Rev. Microbiol. 54:49-79.

Okon Y, Itzigsohn R (1995). The development of *Azospirillum* as a commercial inoculant for improving crop yields. Biotechnol. Adv. 13:415-424.

Okon Y, Labandera-Gonzales C, Lage M, Lage P (2015). Agronomic applications of *Azospirillum* and other PGPR. In. de Brujin FJ (eds.), Biological Nitrogen Fixation. John Wiley and Sons Inc., Hoboken. Pp. 921-933.

Okon Y, Labandera-Gonzalez C (1994). Agronomic applications of *Azospirillum*: an evaluation of 20 years worldwide field inoculation Soil Biol. Biochem. 26:1591-1601.

Ormeño-Orrillo E, Hungria M, Martínez-Romero E (2013). Dinitrogen-fixing prokaryotes. In. Rosemberg E, De Long EF, Lory S, Stackebrandt E, Thompson F (eds.), The Prokaryotes - Prokaryotic Physiology and Biochemistry. Springer-Verlag, Berlin Heidelberg. pp. 427-451.

Pereg L, de-Bashan LE, Bashan Y (2016). Assessment of affinity and specificity of *Azospirillum* for plants. Plant Soil 399:389-414.

Ratcliff WC, Kadam SV, Denison RF (2008). Poly-3-hydroxybutyrate

(PHB) supports survival and reproduction in starving rhizobia. FEMS Microbiol. Ecol. 65:391-399.
Sá JCM, Lal R, Cerri CC, Lorenz K, Hungria M, Carvalho PCC (2017). Low-carbon agriculture in South America to mitigate global climate change and advance food security. Environ. Int. 98:102-112.
Sadasivan L, Neyra CA (1985). Flocculation in *Azospirillum brasilense* and *Azospirillum lipoferum*: Exopolysaccharides and cyst formation. J. Bacteriol. 163:716-723.
Santi C, Bogusz D, Franche C (2013). Biological nitrogen fixation in non-legume plants. Ann. Bot. 111:743-767.
Santos MS (2017). Desenvolvimento de novas formulações de inoculantes líquidos para *Azospirillum brasilense* estirpes Ab-V5 e Ab-V6. Thesis. Londrina, Brasil: Universidade Estadual de Londrina.
Souza RD, Ambrosini A, Passaglia LM (2015). Plant growth-promoting bacteria as inoculants in agricultural soils. Genet. Mol. Biol. 38:401-19.
Stephens JHG, Rask H (2000). Inoculant production and formulation. Field Crops Res. 65:249-258.
Tal S, Okon Y (1985). Production of the reserve material polybetahydroxybutyrate and its function in *Azospirllum brasilense* Cd. Can. J. Microbiol. 31:608-613.
Tittabutr P, Payakapong W, Teaumroonga N, Singletonb PW, Boonkerda N (2007). Growth, survival and field performance of bradyrhizobial liquid inoculants formulations with polymeric additives. Sci. Asia 33:69-77.
Trujillo-Roldán MA, Valdez-Cruz NA, Gonzalez-Monterrubio CF, Acevedo-Sánchez EV, Martínez-Salinas C, García-Cabrera RI, Gamboa-Suasnavart RA, Marín-Palacio LD, Villegas J, Blancas-Cabrera A (2013). Scale-up from shake flasks to pilot scale production of the plant growth-promoting bacterium *Azospirillum brasilense* for preparing a liquid inoculant formulation. Appl. Microbiol. Biotechnol. 97:9665-9674.
Vendan RT, Thangaraju M (2007). Development and standardization of cyst based liquid formulation of *Azospirillum* bioinoculant. Acta Microbiol. Immunol. Hung. 54:167-177.
Watnick P, Kolter R (2000). Biofilm, city of microbes. J. Bacteriol. 182:2675-2679.

academicJournals

Vol. 16(37), pp. 1863-1870, 13 September, 2017
DOI: 10.5897/AJB2017.15968
Article Number: 712AED565991
ISSN 1684-5315

http://www.academicjournals.org/AJB

African Journal of Biotechnology

Full Length Research Paper

Biodegradation and toxicity of waste from anaerobic fermentation of stillage

Mariane Aparecida Messetti[1*], Ariovaldo José da Silva[2], Graciete Mary dos Santos[2], José Silvio Govone[3] and Dejanira Franceschi de Angelis[1]

[1]Department of Biochemistry and Microbiology, Institute of Biosciences, São Paulo State University (UNESP), Av. 24A, n. 1515, Bela Vista, CEP 13506-900, Rio Claro, São Paulo, Brazil.
[2]Department of Sanitation and Environment, Faculty of Agricultural Engineering, State University of Campinas (UNICAMP), Campinas, São Paulo, Brazil.
[3]Department of Statistics, Applied Mathematics and Computation, Institute of Geosciences and Exact Sciences, São Paulo State University (UNESP), Rio Claro, São Paulo, Brazil.

Received 1 March, 2017; Accepted 1 September, 2017

Several studies have been carried out to produce biofuels by anaerobic digestion of stillage from ethanol fermentation. This type of process, known as ABE Fermentation, generates by-products such as acetone, butanol and ethanol. This fermentation can use pure or mixed cultures of anaerobic bacteria, mainly of the genus *Clostridium*. In this context, there is the need for deeper studies for proper disposal of the residue resulting from Anaerobic Fermentation of ethanolic stillage, hereinafter referred to as AF stillage (stillage from Anaerobic Fermentation), obtained after this fermentation. Thus, the aim of this study was to evaluate the biodegradation and toxicity of stillage from Anaerobic Fermentation. The biodegradation of AF stillage in soil samples in the presence and absence of commercial inoculum was evaluated using a respirometric method described by Bartha & Pramer, according to the standard NBR 14283 (ABNT, 1999). The production of CO_2 was evaluated for 57 days. Additionally, quantification of microorganisms was carried out at the beginning and end of the experiment. Toxicity tests were performed with the microcrustacean *Daphnia similis* using raw AF stillage and leachate from the respirometry test, according to the standard NBR 12713 (ABNT, 2009). The results of the respirometry test showed that, after 13 days of incubation, the biodegradation efficiency of all samples was above 30%. Using the Friedman statistical test, results showed that adding the inoculum caused no statistically significant difference in the biodegradation of AF stillage. The acute toxicity tests were performed on raw AF stillage and on the leachates showed that toxicity was removed after biodegradation in soil at all concentrations used. Thus, discharge of AF stillage into soil is an alternative viable disposal.

Key words: Biodegradation, stillage, anaerobic fermentation, toxicity.

INTRODUCTION

Taking into account that ethanol production in Brazil in 2015/2016 was 30.5 billion liters, the production of ethanol stillage was 305 billion liters. Ethanol stillage is characterized as a distillery effluent having a high polluting potential approximately a hundred times more polluting than domestic sewage (CONAB, 2016; Lelis Neto, 2008). Its chemical composition vary depending on the water content, sugarcane characteristics and

fermentation, and distillation processes that were used. In general, stillage presents increased turbidity and low pH, with high levels of organic matter, potassium and calcium, and moderate amounts of nitrogen and phosphorus (Ferraz et al., 1986; Rodella et al., 1983; Tauk, 1987; Gómez and Rodriguez, 2000). According to Fuess and Garcia (2014), currently, almost the whole volume of stillage generated in Brazilian distilleries is directed to the fertigation of sugarcane fields, due to its fertilizer character. In reasonable amounts, fertigation has positive effects on agricultural productivity, acting as a partial or total replacement of mineral fertilizers, especially potassium. However, long-term intensive application of stillage can increase soil salinity (Corazza, 1999), affect sugarcane quality, and also contaminate groundwater (Gonçalves and Silva, 2000). According to Freire and Cortez (2000), stillage can present high levels of chemical oxygen demand (COD) and biochemical oxygen demand (BOD), reaching values up to 210.000 and 100.000 $mg \cdot L^{-1}$, respectively.

According to Green (2011), acetone-butanol-ethanol (ABE) fermentation has been recently reestablished in China. ABE fermentation is one of the oldest micro-biological processes for the commercial production of solvents (Qureshi and Ezeji, 2008). In this type of fermentation, bacteria of the genus, *Clostridium* are used to convert sugars into solvents, and fermentation takes place in two steps. The first step (acidogenesis) is a growth phase in which acetic and butyric acids are rapidly produced, lowering the pH. The second step (solventogenesis) is characterized by acid reassimilation for solvent production. Fermentation also produces carbon dioxide and hydrogen (Green, 2011). The average ABE fermentation time is 36 to 72 h, when approximately 15 to 20 g/L of solvents accumulate, depending on the culture and raw materials used. One of the greatest technological challenges is associated with the low yield of solvents. Choosing microorganisms appropriately is crucial for successful ABE fermentation and for the production of target solvents. Pure cultures (whether natural or mutant) are the most widely used for many scientific studies, since they present a rate of conversion of glucose into solvents within the maximum tolerance limits due to microbial inhibition caused by solvents (Liu and Qureshi, 2009). However, mixed cultures have proven to be more advantageous when complex substrates are used, promoting their degradation by forming integrated communities, in which some species act in a balanced way, or even symbiotically (Santos, 2015).

Although, Brazil finds itself in an advantageous position, especially when it comes to ethanol from sugarcane, the country needs to consolidate its position in the world energy market in a sustainable way, taking into account environmental, economic and social issues (Santos et al., 2011). According to Mello et al. (2007), in the coming years, Brazil will maintain its leading position in the production of ethanol as a result of the natural characteristics of its territory, its large agricultural and industrial experience in the sugar and alcohol sector, and the recent development of biodiesel agribusiness. The expansion of biofuels in Brazil offers great environmental challenges and opportunities, especially for one of the main sources of pollutants from plants, namely stillage. Since there are limits to the use of stillage in fertigation, one of the alternatives is its biodigestion through ABE fermentation.

Improvements in the refining process over time will enable the use of more economical sources of raw materials, such as lignocellulosic biomass and even sugars currently used in ethanol plants. In the latter, only minor modifications would be needed, since bacteria of the genus *Clostridium* are well adapted to utilize sugars derived from cellulosic materials. The production of low cost butanol using lignocellulosic biomass, such as agricultural and forestry waste from biorefineries, has been regarded as a necessary change in order to improve process economy.

Solutions for the stillage generated during the production of ethanol from conventional and cellulosic raw materials were discussed by Wilkie et al. (2000), who supported anaerobic digestion of stillage followed by fertigation. Corazza (1999) described alternative technology that allows stillage to be recycled in the fermentation process, treated in anaerobic reactors, or used in yeast production, animal feed, and even in construction. In this context, reuse of ethanol stillage has been considered as an alternative for the production of biofuels or their byproducts.

Ahn et al. (2011) investigated fermentation for butanol production by *Clostridium pasteurianum* DSM 525 using stillage containing glycerol as a substrate. Glycerol is a byproduct of ethanol fermentation and its concentration in thin stillage ranges from 5.1 to 24.6 g/L (Dowd et al., 1994; Gonzalez et al., 2010; Kim et al., 2008). *C. pasteurianum* DSM 525 is capable of producing butanol using glycerol as the sole source of carbon and energy (Biebl, 2009). Other organic compounds present in thin stillage are lactic and acetic acids, which are mainly produced by bacterial contamination in the ethanol fermentation process (Skinner and Leathers, 2004). The authors found that *C. pasteurianum* DSM 525 was produced from 6.2 to 7.2 g/L of butanol, using glycerol present in stillage as the main source of carbon. The lactic acid in stillage acted as a buffering agent, maintaining the pH of the medium in the range of 5.7 to

*Corresponding author: E-mail: marime7ferreira@gmail.com.

6.1. The results of the study showed the economic viability of butanol production using stillage as a substrate, with the potential to provide all the nutrients that are necessary for fermentation.

In the context of anaerobic digestion of stillage aiming to obtain by-products (ABE fermentation), deeper studies focusing on the final residue obtained after fermentation (AF stillage) are necessary. After removal of the bacterial biomass and separation of the solvents generated in the process, AF stillage is disposed of. Thus, it is appropriate to discuss solutions for proper disposal of AF stillage. Among them, fertigation is a viable alternative. Nonetheless, studies on biodegradation/bioremediation and toxicity are needed for AF stillage correct disposal on soil.

Bioremediation is the use of living organisms, especially microorganisms, to degrade environmental contaminants to less toxic products. The bioremediation process can occur *in situ*, where microorganisms originate from a contaminated area, or *ex situ*, where microorganisms are isolated and transferred to the contaminated site. Contaminating compounds are transformed through the metabolic activity of microorganisms (Vidali, 2001). Microbial diversity in soil plays a key role in this ecosystem. Several scientific papers have demonstrated the role of soil bacteria and fungi in the bioremediation of contaminated areas or even industrial waste. Bio-augmentation involves using microbial consortia capable of degrading the target pollutant. In intrinsic or natural bioremediation, the microorganisms used are autochthonous, that is, native to the site, without any interference of active remediation technologies (Bento et al., 2003).

The respirometric method by Bartha and Pramer (1965) is a technique that is used to determine the biodegradation of organic matter in soil by measuring the amount of CO_2 released into the system. A respirometer acts as a closed system consisting of two interconnected chambers, in which biodegradation of waste and removal of the CO_2 generated during the process take place. This method assumes a correlation between CO_2 production and biodegradation of organic matter (sample) in soil. The efficiency of sample degradation is determined by the amount of CO_2 produced, which allows determining waste stabilization time at different application rates.

Ecotoxicological tests with standard organisms have been used to estimate the toxic effects of certain compounds, providing data for risk assessments in aquatic environments. Among these organisms, micro-crustaceans of the genus *Daphnia* spp. stand out not only because they are easy to grow in a well-controlled laboratory, but also because of their population homogeneity, resulting from parthenogenetic reproduction (Nour et al., 2014).

The aims of this work were: 1) to study the application of AF stillage in soil through respirometry; 2) to carry out microbial quantification at the beginning and end of the test; and 3) to perform toxicity tests using *Daphnia similis.*

Table 1. Physicochemical composition of the AF stillage.

Parameter	Results
pH	7.21
Electrical conductivity (mS/cma)	18.96
Biochemical oxygen demand (BOD) (mg/L)	654
Chemical oxygen demand (COD) (mg/L)	17616
Total organic carbon (TOC) (%)	0.82
Total nitrogen (Kjeldahl) (mg N/L)	0.3
Dissolved oxygen (mg O_2/L)	5.03
Total solids (mg/L)	29288
Fixed solids (mg/L)	15048
Volatile solids (mg/L)	14240
Ashes (%)	1.54
Humidity (%)	97.05
Sulfate (mg SO_4^{-2}/L)	1525
Sulfide (mg S^{-2}/L)	<0.002
Manganese (mg Mn/L)	0.958
Calcium (mg Ca/L)	254
Magnesium (mg Mg/L)	86
Sodium (mg Na/L)	4823
Potassium (mg K/L)	1827
Total phosphate (mg PO_4/L)	156

MATERIALS AND METHODS

Anaerobic fermentation (AF) stillage

The AF stillage is the residue or stillage generated by anaerobic fermentation of ethanol stillage. It was obtained from the Sanitation Laboratory of the Faculty of Agricultural Engineering (FEAGRI/ UNICAMP) and resulted from acetone-butanol-ethanol (ABE) fermentation intended for the production of alcohols and organic acids. For this fermentation, synthetic culture medium was used (Monot et al., 1982 modified by Santos, 2015), supplemented with ethanol stillage and molasses, as well as 1 N NaOH for pH control.

The AF stillage was centrifuged to remove the bacterial biomass. Afterwards, the supernatant recovered was subjected to rotoevaporation in a Marconi rotary evaporator (MA-120) to eliminate the solvents produced during fermentation (acetone, butanol and ethanol). The pressure necessary for the evaporation of the three solvents in a water bath at a temperature between 45 and 50°C (over 404 mm Hg) was taken into account. The AF stillage was then heated at 80°C for 15 min.

The physicochemical properties of the stillage used in this study was characterized according to APHA (1998, 2012) and are shown in Table 1.

Soil sample

The soil used in the respirometry test was collected according to the technical rule L.6.245 from Cetesb (1984), in the geographic coordinates: Latitude -22.39624915/Longitude -47.5431633, localized in the municipality of Rio Claro, in the State of São Paulo,

Table 2. Physical characteristics of the control soil.

Parameter	Grain size distribution (%)					
	Sand				Class	Sub-class
	Thick	Fine	Clay	Loam		
Soil	24.4	11.9	25.9	37.8	Clay	Clay

Table 3. Chemical characteristics of control soil (macro and micronutrientes).

Parameter	Macronutrients (mmolc/dm$^{3)}$ IFSA							V	Relations	
	K	Ca	Mg	H^+Al	Al	SB	CTC	%	Ca/Mg	Mg/K
Soil	4.9	43	15	34	1	63	97	64.9	2.86	3.06
	Micronutrients (mg/dm^3)							pH	OM	P res
	S	Na	Fe	Mn	Cu	Zn	B	$CaCl_2$	g/dm^3	g/dm^3
Soil	8	3	19	26.2	1.4	1.9	0.18	5.5	34	3,0

P, K, Ca, Mg, exchange resin anionic + cationic; Fe, Mn, Ca, Zn: Extractor DTPA-TEA; B, Barium chloride extractor 0.125%; Soil sample was analyzed by Inst. Campineiro de Análise de Solo e Adubo Ltda. (ICASA).

Brazil. These samples were taken from the soil superficial layer of non-contaminated places. Tables 2 and 3 show the physico-chemical characteristics of soil.

Biodegradation test

The biodegradation tests, performed according to the standard NBR 14283 (ABNT, 1999), was used to evaluate changes in CO_2 production in the soil containing AF stillage. Three concentrations of AF stillage in soil (3, 6 and 12%) in the presence and absence of 0.2% commercial inoculum (VCTEC/ByoAct), consisting of a pool of microorganisms isolated from soil, were evaluated. Each treatment included three replicates, according to the protocol; soil; soil + 3% AF stillage; soil + 6% AF stillage; soil + 12% AF stillage; soil + 0.2% inoculum; soil + 0.2% inoculum + 3% AF stillage: soil + 0.2% inoculum + 6% AF stillage; soil + 0.2% inoculum + 12% AF stillage. The respirometers were incubated at 28±2 °C and measurements of the produced CO_2 were performed daily for the first 7 days and at longer intervals for 57 days.

From determination of the amount of biodegradable carbon during the test, the efficiency of biodegradation (EB) was calculated by the equation:

$$EB\% = \frac{\text{Total amount of biodegradable carbon (µmol)}}{\text{Amount of initial organic carbon in soil (µmol)}} \times 100$$

Microbiological analysis of biodegradation test

Heterotrophic bacteria and fungi in the respirometer samples were quantified at the beginning and end of the test. The quantification was performed by plating on Plate Count Agar (PCA) containing actidione (5 ppm) and Sabouraud broth containing chloramphenicol (400 ppm), respectively. Bacterial counts were carried using pour plate technique, and plates were incubated at 35°C for 48 h. Counts for yeasts and molds were performed by spread-plating, and plates were incubated for 5 days at 28°C. The results are given in CFU/g of dry soil.

The same procedure for microbial quantification was carried out for the commercial inoculum and AF stillage. The results obtained are expressed as CFU/ml.

Toxicity tests

Leachates from the samples in the respirometers were prepared at the beginning and end of the test, at a concentration of 10% in distilled water. The solutions were stirred in a shaker for 30 min and then decanted for 7 days, at room temperature. The supernatant was used in acute toxicity tests with the microcrustacean *D. similis* according to the standard NBR 12713 (ABNT, 2009), as well as raw AF stillage.

Statistical analysis

The Friedman test (Zar, 1999), which is a nonparametric test, was used to analyze the results from the respirometric biodegradation test and the quantification of microorganisms. The level of significance was 5%. The results of the toxicity tests with *D. similis* were calculated from statistical analysis carried out by the Trimmed Spearman-Karber method using the software JSPEAR (Hamilton et al., 1977).

RESULTS AND DISCUSSION

Biodegradation test

The occurrence of biodegradation was observed in all respirometers, which was evidenced by the production of CO_2. It was observed that microbial activity was not affected by the addition of AF stillage, since the amount of cumulative CO_2 increased as the concentration of

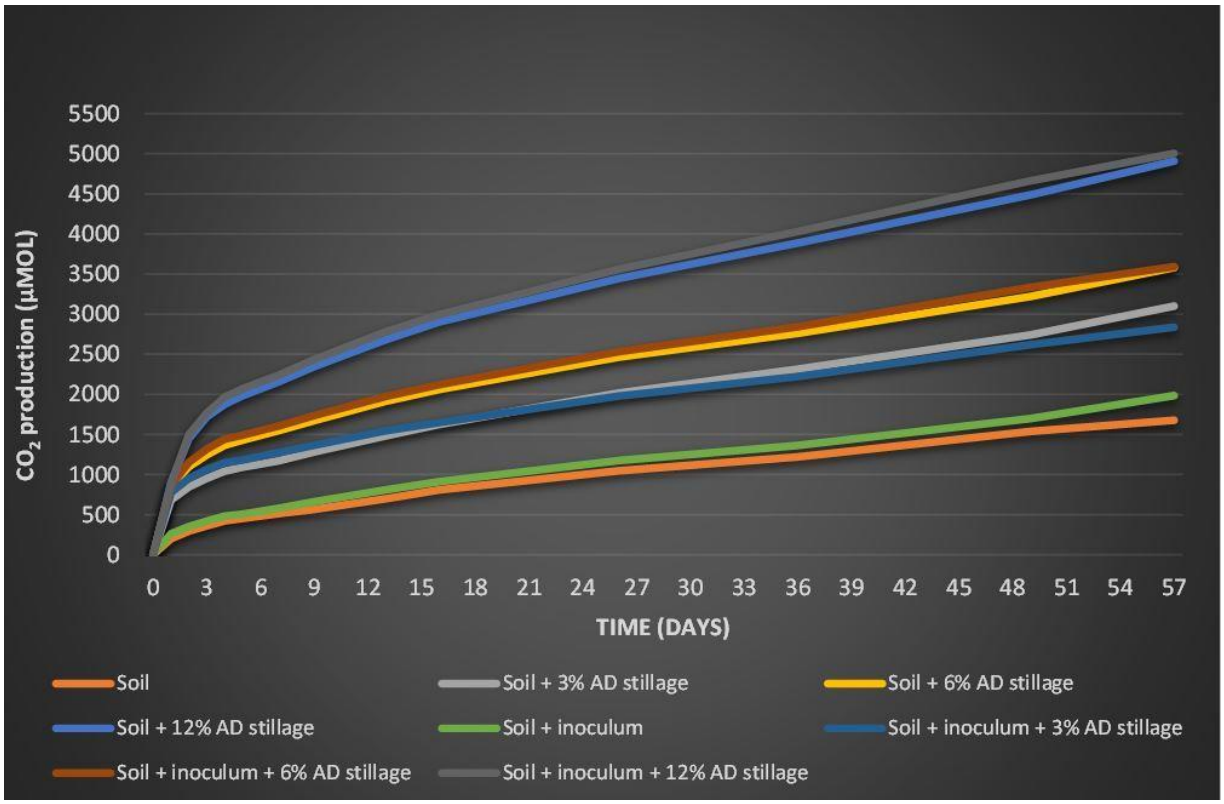

Figure 1. Cumulative production of CO_2 in different treatments in the respirometry test with AF stillage.

residue (AF stillage) increased (Figure 1). The statistical analysis of the data on the daily production of CO_2 (µmol) using the Friedman test revealed that adding the inoculum did not cause significant differences (with a significance level of 5%) as compared to control soil and AF stillage at the concentrations of 6 and 12% (P-values of the probability tests: p=0.13, 0.78 and 0.98, respectively). There was statistical difference only between soil with 3% AF stillage and the same sample supplemented with inoculum (p=0.047).

Almeida et al. (2013) also found similar results in a respirometry test, in which a commercial inoculum was added to help with the biodegradation of ethanol stillage. The results for clayey soil showed that the curves of CO_2 production were very similar in the presence and absence of inoculum. The authors concluded that the addition of the inoculum did not affect stillage biodegradation positively.

Adding the three concentrations of AF stillage to the soil had a significant effect (p<0.0001) with respect to the daily production of CO_2 (µmol); also, adding 6 and 12% AF stillage to the soil containing inoculum had significant effect (p=0.0039 and p<0.0001, respectively). There was no difference between adding AF stillage to the soil at the concentrations of 3 and 6% (p=0.47), but both were different from 12% AF stillage (p=0.003 and 0.0041, respectively). For the soils supplemented with inoculum, the three concentrations of AF stillage were different from each other (p=0.0154, p<0.0001 and p=0.0015, respectively, for comparisons between 3 and 6; 3 and 12; and 6 and 12%).

Efficiency of biodegradation

Table 4 shows that after 13 days, all the samples presented biodegradation efficiency above 30%. This result is significant, since there is a Brazilian technical standard that establishes a minimum biodegradation efficiency of 30% for waste disposal on soil (NBR 14283) (ABNT,1999). At the end of 57 days, the highest efficiency was observed for the sample containing soil with 3% AF stillage (92.64%), followed by sample containing soil + inoculum + 3% AF stillage (75.52%). In Figure 1, the same samples presented the lowest amount of cumulative CO_2; however, their efficiency at the start of incubation was above 30%. The samples containing soil + 6% AF stillage reached this value on the 3rd and 4th day in the presence and absence of inoculum, respectively. The samples containing soil + 12% AF stillage reached this value on the 9th and 13th day in the presence and absence of inoculum, respectively. Although its addition did not lead to statistically significant differences, samples with inoculum reached 30%

Table 4. Efficiency of biodegradation of AF stillage in the respirometry test for 57 days.

Days	Samples					
	Soil + 3% AF stillage	Soil + 6% AF stillage	Soil + 12% AF stillage	Soil + inoculum + 3% AF stillage	Soil + inoculum + 6% AF stillage	Soil + inoculum + 12% AF stillage
0	0.00	0.00	0.00	0.00	0.00	0.00
1	31.32	21.44	11.42	37.46	21.70	11.18
2	35.88	26.14	18.80	42.81	27.91	19.61
3	38.46	28.76	22.09	45.82	31.13	22.94
4	40.30	30.64	23.65	47.21	33.20	25.12
5	41.59	31.75	24.89	47.42	33.80	26.31
7	42.69	33.60	26.73	49.41	35.52	28.07
9	46.61	35.98	28.94	51.99	38.09	30.42
13	50.95	39.53	32.25	55.18	41.48	33.89
16	53.15	40.77	34.07	54.69	42.70	35.58
26	63.09	46.11	39.00	60.62	48.34	40.89
36	71.18	50.16	43.38	65.27	52.82	45.73
49	78.20	54.66	47.95	70.31	58.43	50.81
57	92.64	61.95	52.54	75.52	62.27	54.12

Table 5. Initial and final counts of heterotrophic bacteria and fungi from the respirometry test, expressed in colony forming units per gram of soil (CFU/g).

Samples	Bacteria (10^5 CFU/g)		Fungi (10^2 CFU/g)	
	Initial	Final	Initial	Final
Soil	3.4	23.5	4.7	36.0
Soil + 3% AF stillage	35.7	26.5	7.9	33.0
Soil + 6% AF stillage	67.5	44.5	11.1	31.5
Soil + 12% AF stillage	132.4	45.0	17.6	38.0
Soil + inoculum	153.4	11.0	7.7	49.0
Soil + inoculum + 3% AF stillage	185.7	39.5	10.9	41.0
Soil + inoculum + 6% AF stillage	217.9	18.5	14.1	25.5
Soil + inoculum + 12% AF stillage	282.4	109.5	20.6	33.0

biodegradation efficiency in a shorter time.

Microbiological analysis of biodegradation test

Table 5 indicates that the initial bacterial and fungal counts in the control soil were 3.4×10^5 and 4.7×10^2 CFU/g, respectively, while addition of the inoculum increased these values. In the inoculum, the load of bacteria was 1.5×10^7 CFU/ml, and the concentration of fungi was 3×10^2 CFU/ml.

The number of microorganisms was also proportionally higher with the addition of 3, 6 and 12% AF stillage, in which the number of bacteria was 1.08×10^8 and that of fungi was 1.08×10^4 CFU/ml. There were some variations in the final quantification. At the end of the test, the overall number of bacteria was lower than in the initial plating. This was probably due to the intense metabolic activity of microorganisms during the test, with consequent depletion of the nutrients present. On the other hand, there was an increase in the fungal count (CFU/g) at the end of the experiment. It is worth noting that fungi were present in a smaller amount at the beginning of the test. The Friedman test showed significant differences between the initial and final number of microorganisms, both for bacteria and fungi ($p<0.05$).

Toxicity tests

The acute toxicity test on *D. similis* was performed according to NBR 12713 method (ABNT, 2009). The results showed acute toxicity, with an EC_{50} of 9.10% and approximately 11 toxic units (TU) for the raw AF stillage studied (Table 6). This result indicates that AF stillage at a concentration of 9.10% is potentially toxic to aquatic organisms. The same test was carried out with leachate

Table 6. Results of the acute toxicity test on *D. similis* for raw AF stillage.

EC(50) (%)	Toxic units (TU)
9.10	10.99

EC(50), Median effective concentration = sample concentration that causes acute effects (mortality or immobility) to 50% of the organisms within a given period of exposure under the test conditions. TU = toxic units = 100/EC(50).

Table 7. Results of the acute toxicity test on *D. similis* performed with leachate using respirometry test.

Samples	Toxicity (toxic units)	
	Initial	Final
Soil	NT	NT
Soil + 3% AF stillage	1.0	NT
Soil + 6% AF stillage	1.2	NT
Soil + 12% AF stillage	NT	NT
Soil + inoculum	NT	NT
Soil + inoculum + 3% AF stillage	1.2	NT
Soil + inoculum + 6% AF stillage	1.7	NT
Soil + inoculum + 12% AF stillage	NT	NT

NT = non-toxic.

from the samples in the respirometers, at the beginning and end of the test, for both experiments.

In Table 7, it is shown that leachate from the controls used in the respirometry test showed no acute toxicity to *D. similis* (soil and soil + inoculum), at the beginning and end of the test. In the beginning of the respirometry test, changing AF stillage addition from 3 to 6% increased the toxicity of the samples, both in the presence and absence of inoculum, which can be verified by the increase of UT values. However, samples containing AF stillage 12% showed no toxicity, in the presence and absence of inoculum.

One possible explanation would be that the leachates were decanted for 7 days at room temperature, and during that time, existing microorganisms in AF stillage were able to biodegrade compounds that could be toxic to *D. similis*. Thus, the supernatant of these leachates showed no toxicity since the amount of microorganisms present in the soil after addition of 12% AF stillage was higher than that present in the other concentrations (Table 5).

At the end of the respirometry test, in which AF stillage underwent biodegradation, the leachate samples showed no toxicity. These results are similar to those obtained by Quiterio (2013) who found that raw ethanol stillage was extremely toxic to *D. similis*. However, after biodegradation in soil quantified with the respirometric technique, toxicity was removed.

Conclusion

In the respirometry test, it was observed that addition of the commercial inoculum caused no statistically significant difference in the biodegradation of AF stillage. In the absence of inoculum, the two lowest concentrations were not different from each other; there were differences only with the addition of AF stillage at a concentration of 12%. This shows that it may be necessary to use the minimum concentration for the biodegradation process to be more efficient, since the minimum efficiency of 30% was reached on the 13th day when 12% AF stillage was used, while the same efficiency was reached on the 1st day when 3% AF stillage was used.

The acute toxicity tests showed that raw AF stillage was extremely toxic to *D. similis.* However, after the biodegradation process, toxicity was removed. Thus, disposal of AF stillage on soil becomes a viable option, since it did not show potential toxicity to aquatic organisms in the case of groundwater contamination and it presented a minimal biodegradation efficiency of 30%, as recommended by the Brazilian technical standard for waste disposal on soil.

CONFLICT OF INTERESTS

The authors have not declared any conflict of interests.

ACKNOWLEDGEMENT

This work was supported by the National Council for Scientific and Technological Development (CNPq).

REFERENCES

Associação Brasileira de Normas Técnicas (ABNT) (1999). NBR 14.283 Resíduos em solo – Determinação da biodegradação pelo método respirométrico.

Associação Brasileira de Normas Técnicas (ABNT) (2009). NBR 12713 Ecotoxicologia Aquática - Toxicidade aguda - Método de ensaio com *Daphnia* spp. (Crustacea, Cladocera).

Ahn JH, Sang BI, Um Y (2011). Butanol production from thin stillage using *Clostridium pasteurianum*. Bioresour. Technol. 102:4934-4937.

Almeida NC, Tomasella RC, Govone S, Kinjo S, Angelis DF (2013). Study of stillage biodegradation by respirometry in sandy and clay soils. Afr. J. Agric. Res. 8(35):4506-4513.

APHA Standard methods for the examination of water and wastewater (1998). Washington, DC, USA: American Public Health Association/American Water Works Association / Water Environment Federation. 20. ed.

APHA Standard methods for the examination of water and wastewater (2012). Washington, DC, USA: American Public Health Association/American Water Works Association / Water Environment Federation, 2012. 22. ed.

Bartha R, Pramer D (1965). Features of flask and method for measurement of the persistence and biological effects of pesticides in soil. Soil Sci. 100(1):68-70.

Bento FM, Camargo FAO, Okeke B (2003). Bioremediation of soil contaminated by diesel oil. Braz. J. Microbiol. 34(1):65-68.

Biebl H (2001). Fermentation of glycerol by *Clostridium pasteurianum* –

batch and continuous culture studies. J. Ind. Microbiol. Biotechnol. 27(1):18-26.
Cetesb (Companhia Ambiental Do Estado De São Paulo) (1984). Norma técnica L. 6.245 – Coleta e preparação de amostras. Procedimentos, São Paulo, 25 p.
COMPANHIA NACIONAL DE ABASTECIMENTO (CONAB) (2016). Acomp. safra bras. cana. Quarto levantamento, Brasília 2(4):1-76.
Corazza RI (1999). Reflexões sobre o papel das políticas ambientais de ciência e tecnologia na modelagem de opções produtivas 'mais limpas' numa perspectiva evolucionista: um estudo sobre o problema da disposição da vinhaça. In. III Encontro Nacional da Sociedade Brasileira de Economia Ecológica, Recife.
Dowd MK, Johansen SL, Cantarella L, Reilly PJ (1994). Low molecular weight organic composition of ethanol stillage from sugarcane molasses, citrus waste, and sweet whey. J. Agric. Food Chem. 42(2):283-288
Ferraz CAM., Aquarone E, Krauter M, Balloni W, Florenzano G (1986). Utilização de subprodutos da indústria alcooleira na obtenção de biomassa de *Spirulina maxima.* Parte II. Emprego do resíduo da destilação do mosto fermentado (vinhaça). Rev. Microbiol. 17:15-25
Freire WJ, Cortez LAB (2000). Vinhaça de cana-de-açúcar. Guaíba: Agropecuária, 203 p.
Gómez J, Rodríguez O(2000). Effects of vinasse on sugarcane (*Saccharum officinarum*) productivity. Rev. Fac. Agron. (LUZ). 17:318-326
Gonçalves CAS, Silva EL (2000). Tratamento Físico-Químico da Vinhaça. In. XXVII Congresso Interamericano de Engenharia Sanitária e Ambiental. Associação Brasileira de Engenharia Sanitária e Ambiental – ABES. Fortaleza - CE, Brazil.
Gonzalez R, Campbell P, Wong M (2010). Production of ethanol from thin stillage by metabolically engineered *Escherichia coli*. Biotechnol. Lett. 32(3):405-411.
Green EM (2011). Fermentative production of butanol - the industrial perspective. Curr. Opin. Biotechnol. 22:1-7.
Hamilton SL, Mclaughlin M, Karlin A (1977). Disulfide bond cross-linked dimmer in acetylcholine receptor from *Torpedo californica*. Biochem. Biophys. Res. Commun. 79:692-699.
Kim Y, Mosier NS, Hendrickson R, Ezeji T, Blaschek H, Dien B, Cotta M, Dale B, Ladisch MR (2008). Composition of corn dry-grind ethanol by-products: DDGS, wet cake, and thin stillage. Bioresour. Technol. 99(12):5165-5176.
Lelis Neto JA (2008). Monitoramento de componentes químicos da vinhaça aplicados em diferentes tipos de solo. 88p. Dissertação de Mestrado em Agronomia, Área de concentração: Irrigação e Drenagem – Escola Superior de Agronomia "Luiz de Queiroz", Universidade de São Paulo, Piracicaba.
Liu S, Qureshi N (2009). How microbes tolerate ethanol and butanol. New Biotechnol. 26(3):117-121.
Mello EB, Canepa EL, Costa MM (2007). Visões Ambientais para o Financiamento de Biocombustíveis no Brasil. In. A Expansão da Agroenergia e seus Impactos sobre os Ecossistemas Naturais Brasileiros, Anais. Rio de Janeiro: FBDS, CIB, BNDES. Disponível em: <http://www.fbds.org.br/fbds/Apresentacoes/13_%20Eduardo_Bandeira_de_Mello_BNDES.pdf >Acesso em: abr 2013.
Monot F, Martin J, Petitdemange H, Gay R (1982). Acetone and butanol production by *Clostridium acetobutylicum* in a synthetic medium. Appl. Environ. Microbiol. 44(6):1318-1324.
Nour EAA, Candello FP, Dos Santos EMR, Barretto AS, Domingues LM (2014). Tratamento biológico de formaldeído: toxicidade residual monitorada por bioensaios com *Daphnia similis*. Ecotoxicol. Environ. Contamin. 9(1):77-85.
Quiterio GM (2013). Avaliação do processo de biodegradação da vinhaça no solo mediante adição do biofertilizante. Dissertação de Mestrado em Tecnologia, Área de concentração: Tecnologia e Inovação - Faculdade de Tecnologia da Universidade Estadual de Campinas, Limeira.
Qureshi N, Ezeji TC (2008). Butanol, "a superior biofuel" production from agricultural residues (renewable biomass): recent progress in technology. Biofuels Bioproducts Biorefining 2(4):319-330.
Rodella AA, Zambello Júnior E, Orlando Filho J (1983). Effects of vinasse added to soil on pH and exchangeable aluminum content. In. Congress of the International Society of Sugar Cane Technologists, 1983, Havana. Proceedings. Havana: Universidad de La Habana: pp. 189-214.
Santos GM (2015). Efeito da vinhaça na produção biológica de álcoois e ácidos orgânicos voláteis por meio de consórcio microbiano. Dissertação de Mestrado em Engenharia Agrícola, Área de concentração: Água e Solo – Faculdade de Engenharia Agrícola da Universidade Estadual de Campinas (FEAGRI), Universidade Estadual de Campinas, Campinas.
Santos MFRF, Borschiver S, Couto MAPG (2011). O complexo agroindustrial da cana-de-açúcar no Brasil: uma discussão sobre aspectos atuais relacionados ao etanol biocombustível. In. Economia & Tecnologia/ Centro de Pesquisas Econômicas (CEPEC); Programa de Pós-Graduação em Desenvolvimento Econômico (PPGDE); Universidade Federal do Paraná (UFPR). 24:145-158.
Skinner KA, Leathers TD (2004). Bacterial contaminants of fuel ethanol production. J. Ind. Microbiol. Biotechnol. 31(9):401-408.
Tauk SM (1987) Efeito de doses cumulativas de vinhaça em algumas propriedades do solo sob cerrado e do solo de culturas do milho e cana-de-açúcar no município de Corumbataí, SP. Tese (Livre-docência), Instituto de Biociências, Universidade Estadual Paulista, Rio Claro, São Paulo, Brazil.
Vidali M (2001). Bioremediation. An overview. Pure Appl. Chem. 73(7):1163-1172.
Wilkie AC, Riedesel KJ, Owens JM (2000). Stillage characterization and anaerobic treatment of ethanol stillage from conventional and cellulosic feedstocks. Biomass Bioenergy 19:63-102.
Zar JH (1999). Biostatistical Analysis, Prentice Hall, EUA, 4ª ed.

academicJournals

Vol. 16(37), pp. 1871-1881, 13 September, 2017
DOI: 10.5897/AJB2017.16122
Article Number: 4EEAB8765993
ISSN 1684-5315

http://www.academicjournals.org/AJB

African Journal of Biotechnology

Full Length Research Paper

Objective assessment of bull sperm motility parameters using computer vision algorithms

Daniel Rodríguez-Montaña[1] and Edgar Roa-Guerrero[1,2*]

[1]Departamento de ingeniería, semillero de investigación KINESTASIS, Universidad de Cundinamarca, Colombia.
[2]Departamento de ingeniería, grupo de investigación GITEINCO, Universidad de Cundinamarca, Colombia.

Received 20 June, 2017; Accepted 8 September, 2017

The quality control of frozen semen samples from cattle is established by parameters such as percentage of progressive motility (% MP) because it is related to the fertilization capacity of bulls. Nowadays, sperm quality test is performed by direct visual inspection of sperm through a microscope in andrology laboratories. However, there is a high subjectivity in the observation and assessment depending on the observer; thus, causing unreliable diagnoses and non-repetitiveness in results. The development of a low cost computer tool was proposed to identify the individual sperm motility in cattle through the application of artificial vision algorithms. The methodology consisted of: the acquisition and pre-processing of videos obtained from thawed cryopreserved samples, the segmentation, filtering and detection of spermatozoa using the Fisher Discriminant Analysis and Adaptive Gaussian Models, followed by the assignment and construction of sperm trajectories through the Munkres Algorithm and Kalman Filter. Finally, the characterization and assessment of sperm motility parameters were performed based on the criteria present in computer-aided semen analysis (CASA) commercial systems. The results obtained showed high correlation for the individual sperm motility with a determination coefficient of 0.8143 for 10 different samples of bull sperm with respect to manual analysis. Likewise, a concordance coefficient of 0.966 was found in the 95% confidence interval using the Bland-Altman test, indicating that the measures were highly similar. In this way, the methodology is a reliable technological support that contributes to the improvement of quality control of semen samples from cattle.

Key words: Sperm motility, track detection, fisher discriminant analysis, Gaussian models, Kalman filter.

INTRODUCTION

In Colombia, agricultural activity and majority of the bovine livestock have a great impact on the internal economy of the national territory (DANE, 2016). The country has a large cattle market and, therefore, a demanding commercialization of semen straws of cattle. One of the most important aspects is the sperm quality because there is a high demand of bovine semen straws for artificial insemination processes (Livestock Context,

*Corresponding author. E-mail: eeduardoroa@ucundinamarca.edu.co. Tel: 314 5482 315. Fax: (+57 1) 828 1483. Ext: 142.

2017).

Nowadays, semen analysis is usually done manually through physical observation of spermatozoa under the microscope by specialists in andrology for a long time period (World Health Organization, 2010). However, this conventional procedure can have errors due to factors such as: subjectivity in the determination of progressive and non-progressive moving spermatozoa, lack of repetitiveness in the results and ocular fatigue of the expert for long working hours, thus, affecting the result of the analysis and the objective determination of the bull fertility (Hidalgo et al., 2017). On the other hand, commercial systems of computer-aided semen analysis (CASA) (Lu et al., 2014) have been developed, which allow the identification of seminal parameters with automatically high precision. However, these systems are closed and expensive, hence their implementation is not common in the livestock sector. Although in Colombia, only the case of one commercial system is reported, researchers have already developed algorithms to determine sperm parameters and its relation with semen quality, as well as detection of velocities of cells by CASA (Nagy et al., 2015).

The main objective of this research was to develop a methodology that reduces errors in the results of sperm motility analysis, by implementing a computational tool that performs artificial vision techniques on recorded videos, to provide the specialist, a support technology based on results obtained objectively and makes it to be easily adaptable to many different laboratories.

The methodology implemented consists of four phases in general; phase 1 is the acquisition and pre-processing of the videos through a Leica DM500 led binocular microscope, phase 2 is the segmentation and extraction of motile and non-motile spermatozoa. Subsequently, in phase 3, the algorithm was implemented to assign detections and construct trajectories described by the spermatozoa in the video. Finally, the proposed method analyzes these trajectories of the spermatozoa and identifies the sperm motility parameters following the protocols established by the OMS manual.

In the present investigation, there is a report on the development results, implementation and validation of the computational tool for individual sperm motility assessment in bovines from videos of semen samples obtained from 10 specimens.

MATERIALS AND METHODS

Initially, preparation of the seminal samples was performed according to established protocols in andrology and veterinary medicine laboratories (Vincent et al., 2012). Considering that, this procedure can influence the results of the motility analysis (Contri et al., 2010). In the investigation, the authors only worked on samples of frozen semen for each breed of bull (white black ear), the frozen samples were withdrawn from the liquid nitrogen vessel, each straw was thawed by a water bath for 60 s and 5 µL of semen were placed on a preheated slide at 37°C. Subsequently, the videos were captured using a Leica DM500 led binocular microscope, with digital camera Wi-Fi model ICC50W attached to the lens for different objectives.

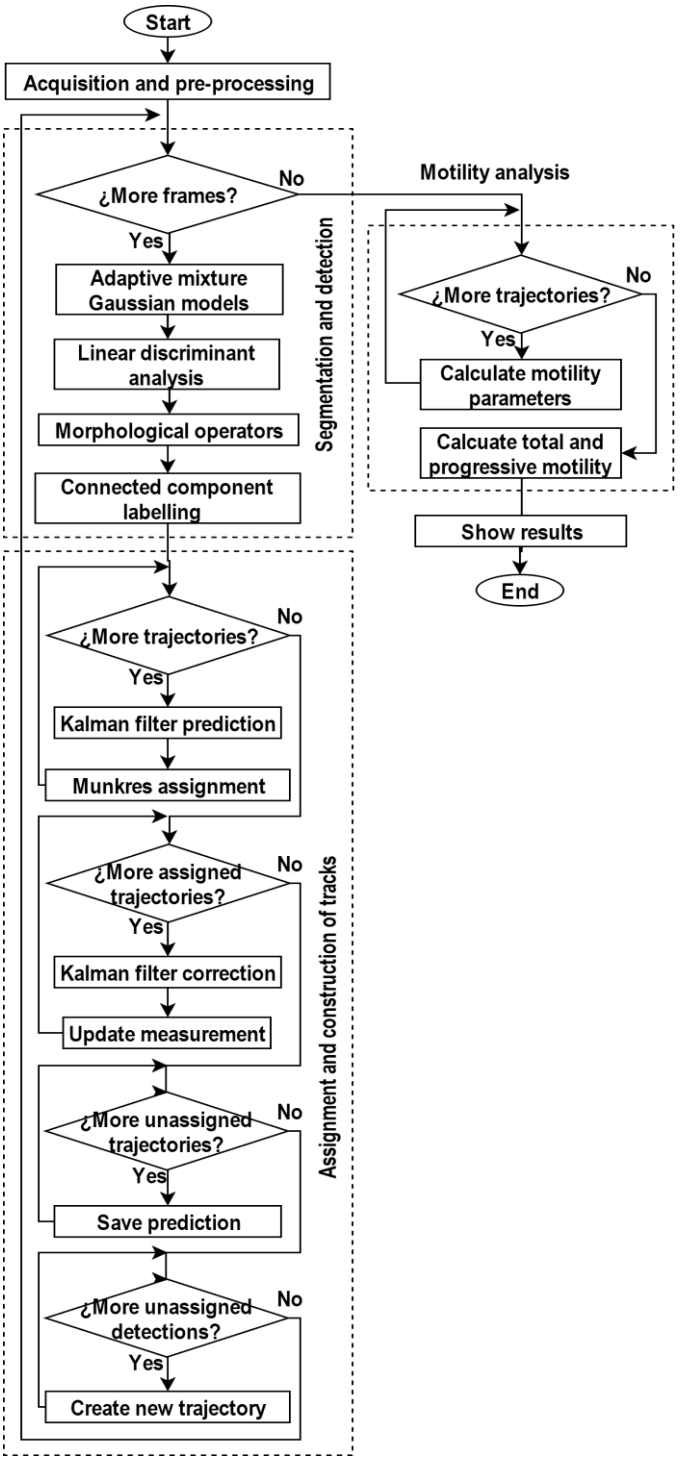

Figure 1. Proposed methodology.

The proposed methodology for the identification of individual sperm motility consists of 4 phases, as shown in Figure 1. In the first phase, video acquisition and pre-processing of the video were performed. In the second phase, the segmentation and detection of spermatozoa in motion were performed through adaptive Gaussian

models. Subsequently, in the third stage, the allocation and construction of trajectories were performed. Finally, validation of the computational tool was performed through sperm motility indexes. Each of the four phases implemented are described below.

Acquisition and pre-processing

When the sample with 5 µL of semen was prepared on a slide and covered with a coverslip, it was focused with a 40x eyepiece using the Leica DM500 led binocular microscope made in Germany and a laptop with Intel core i5 processor and 4 GB memory ram, respectively. Afterwards, the camera software obtained the videos that were later stored in a computer, with the following attributes. Format: WMV; resolution: 640 x 480 pixels; frame rate: 30 Hz; data rate: 1572 kbp; duration: 5 s.

After obtaining the videos, a pre-processing stage was applied which allowed adjusting the contrast of the frame in order to increase the difference between light and dark pixels, thus improving the performance of the segmentation process.

Segmentation and detection of spermatozoa

For extraction of the spermatozoa, a similar technique of frame differentiation was used as developed by Stauffer and Grimson (1999), called adaptive background Gaussian models, with comparison of the value of each pixel with respect to Gaussian functions that are modeled adaptively. It is important to define the probability of each pixel belonging to a background image region. The variance of the pixel values over time allows the modeling of Gaussian functions present in an image. Therefore, these models make prediction possible when a particular pixel is part of a moving object or the background of the image. The probability of observing the pixel value is obtained from Equation 1:

$$P(X_t) = \sum_{i=1}^{K} \omega_{i,t} * \eta(X_t, \mu_{i,t}, \Sigma_{i,t}) \quad (1)$$

Where, K is the number of Gaussian models, ω is an estimated weight coefficient for a model i per unit of time t. The variable η represents the conventional Gaussian probability density, where X_t takes the value of the pixels in the image. µ is the mean value and Σ is the covariance existing in the combination of models. Likewise, by Equation 2, Gaussian probability density was determined adaptively, allowing differentiation of objects that have motion on a video.

$$\left(X_t, \mu_{i,t}, \Sigma_{i,t}\right) = \frac{1}{\frac{n}{2\pi^{\frac{n}{2}}|\Sigma_{i,t}|^{\frac{1}{2}}}} * e^{-\frac{1}{2}\left(X_t-\mu_{i,t}\right)^T \Sigma_{i,t}{}^{-1}\left(X_t-\mu_{i,t}\right)} \quad (2)$$

Where, *n* is the domain size of the normal distribution.

Since the resulting binary image exhibits in most cases, unwanted particles and objects due to the movement of the seminal sample, it is necessary to carry out a filtering step in order to optimize the image and prevent further erroneous detections in the following process stages (Maintz, 2005). Later, an analysis of connected components was implemented in order to recognize the regions of the binary image and to develop an analysis of their geometric parameters (Gonzalez and Woods, 2008), in which fundamental data such as area and center of mass (centroid) are abstracted. The centroid denotes the coordinate on the image which is located in the region of pixels of interest, which in this case, would correspond to the head of a spermatozoon.

Considering that the adaptive Gaussian modeling method can only segment spermatozoa in motion, the linear discriminant analysis method described by Bishop (2016) aims to segment all the spermatozoa present in the frames, regardless of whether they are in motion or not, in order to determine the total motility of the sample. This analysis allows the classification of data between two or more classes. Its function is to maximize inter-class variance and minimize intra-class variance. In this way, a discriminant vector is created to maximize the variance between the pixels belonging to the bottom of the head of a spermatozoon by Equations 3 and 4.

$$S_B = \sum N_C(\mu_C - \mu)(\mu_C - \mu)^T \quad (3)$$

$$S_W = \sum N_{i \in C}(x_i - \mu_C)(x_i - \mu_C)^T \quad (4)$$

Where, µ is the mean of all pixels, µc is the mean of each class, N_C is the number of patterns in the class and x_i is the value of each pixel. Subsequently, the discriminant vector is obtained with Equation 5 that separates the two classes and allows segmentation.

$$J(W) = \frac{W^T.S_B.W}{W^T.S_W.W} \quad (5)$$

Assignment and construction of trajectories

When applying the segmentation algorithm to the video, multiple sperm detections are evident in each frame. These must be interpreted and organized under a set of real trajectories, in order to ensure that different detections correspond to a common trajectory along the frames and, in this way, registering a record of the coordinates of each moving target.

The assignment and construction of the tracks followed by the spermatozoa are developed at first through the application of Munkres assignment algorithm, followed by a Kalman filter. The first technique corresponds to variation of the assignment algorithm of Munkres (1957). This mathematical model aims to make a direct assignment of *m* elements to *n* destinations by means of an *m* x *n* matrix called the cost matrix. These costs are values related to the probability of assigning an element of row *m* to one of column *n* whose total cost is minimal.

Where *m* represents the detections in the binary image, *n* represents the sperm trajectories and each element of the matrix relates to the difference between estimated position and the actual position of the sperm. On the other hand, the Kalman filter is a set of mathematical equations that provide efficient computational means to estimate the state of a process, in such a way that it minimizes the mean square error. This filter allows estimations of states in past, present and even future. This algorithm was designed by Kalman (1960) which describes its operation as a predictive and corrective cycle that communicates with each other through a feedback. In Equations 6 and 7, the Kalman filter prediction stage is described in discrete time:

$$\hat{x}_k^- = A\hat{x}_{k-1} + Bu_k \quad (6)$$

$$P_k^- = AP_{k-1}A^T + Q \quad (7)$$

Where, $\hat{x}_k^-$ is the current state prediction, $\hat{x}_{k-1}$ represents the previous state prediction, u_k is the position measurement, A and B are state transfer matrices, P_k^- is the error covariance *a priori* and Q is the process noise covariance. Subsequently, the position is updated through the correction stage described by Equations 8, 9 and 10, which consist of obtaining new measurements of the state variable and its conjugation with the *a priori* estimation of the prediction.

$$K_k = P_k^- H^T (HP_k^- H^T + R)^{-1} \quad (8)$$

$$\hat{x}_k = \hat{x}_k^- + K_k(z_k - H\hat{x}_k^-) \quad (9)$$

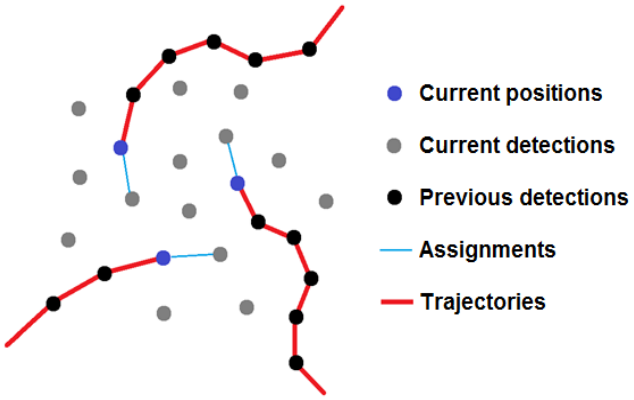

Figure 2. Representation of the assignment of sperm detections to their trajectories.

$$P_k = (I - K_k H)P_k^- \quad 10$$

Where, K_k is the Kalman gain, *H* is the measurement state matrix, *R* is the covariance of the measurement error and z_k is the current system measurement.

In this way, the positions that define the trajectories of the spermatozoa are determined, considering both the observed measurements and the coordinates estimation. All previous measurements constitute a criterion for predicting future measurements. The correction, in turn, updates the data and incorporates it into the information history through a feedback loop. In the cost matrix, the difference between the current position measurement and the Kalman prediction is stored, and eventually, a given detection is assigned with a greater probability of belonging to a real trajectory, as shown in the Figure 2.

The first detections presented in the initial frame of a video are classified in initial positions of trajectory and the unassigned detections become a new trajectory. In the case of the assigned detections, the update of the measurement in each frame is given by assigning a new element to the track. On the other hand, those tracks that do not comply with a minimum number of points are automatically deleted by the algorithm, because they are insignificant or indicate a detection error.

Characterization of sperm motility

Finally, the trajectory of the spermatozoon is defined by means of a matrix that represents the coordinates X and Y of the positions through time within the image, which allows determination of the most common parameters of sperm motility as realized in the systems CASA (Agarwal and Sharma, 2017) which have: curvilinear velocity (VCL), average velocity (VAP), straight line velocity (VSL), linearity index (LIN), straightness index (STR), wobbling index (WOB), percentage of total motility (% MT) and progressive motility (% MP).

The curvilinear velocity is a fundamental parameter in individual sperm motility. The other parameters are calculated from this value. The total distance was obtained by summing the distances between each coordinate *k* in the space of the image and its multiplication by a factor (A) that converts Cartesian coordinates (x_1, y_1) into micrometers dominion (*μm*). The velocity was determined in Equation 11 by multiplying the total distance by the capture frequency of the video F (s^{-1}) as follows:

$$VCL = A * F * \sum_{i=1}^{k} \sqrt{(x_2 - x_1)^2 + (y_2 - y_1)^2} \quad 11$$

Because the average velocity corresponds to the smoothed real trajectory, a mean filter was applied for each column of the coordinate matrix and subsequently computed. Mathematically, the sequential mean was calculated for each element of the column vector (X_i, Y_i), obtaining another average column vector (M_i, N_i) as shown in Equations 12 and 13. Then, the same equation previously used was applied, but adapted to the ne values (Equation 14):

$$M_i = \frac{\sum_i X}{i} \quad 12$$

$$N_i = \frac{\sum_i Y}{i} \quad 13$$

$$VAP = A * F * \sum_{i=1}^{k} \sqrt{(m_2 - m_1)^2 + (n_2 - n_1)^2} \quad 14$$

Also, the rectilinear velocity was computed from the initial point (x_i, y_i) to the final point (x_f, y_f) of the trajectory described by the spermatozoon, and likewise using Equation 15, the velocity was converted to units of *μm/s*:

$$VSL = A * F * \sqrt{(x_f - x_i)^2 + (y_f - y_i)^2} \quad 15$$

Subsequently, the linearity indices were calculated in Equation 16, straightness in Equation 17 and wobbling in Equation 18:

$$LIN = \frac{VSL}{VCL} \quad 16$$

$$STR = \frac{VSL}{VAP} \quad 17$$

$$WOB = \frac{VAP}{VCL} \quad 18$$

Moreover, a characterization stage was designed in order to classify each spermatozoid into a motility category depending on its speed and trajectory. Finally, the percentages of total motility and progressive motility are determined by Equations 19 and 20, being the progressive motility percentage and one of the most important descriptors of the quality of a seminal sample as described in Vincent et al. (2012).

The criterion implemented for the classification of sperm motility in the categories of fast progressive (grade A), slow progressive (grade B), non-progressive (grade C) and non-motile (grade D) was based on criteria implemented in CASA systems for the analysis of frozen samples of bovine semen. However, the thresholds used for the classification were previously characterized, considering the specific conditions of our design, since for CASA systems, there is no official standard (Simonik et al., 2015).

$$\%MT = \frac{A+B+C}{Total} \quad 19$$

$$\%MP = \frac{A+B}{Total} \quad 20$$

RESULTS

Acquisition and pre-processing

The first phase tested was the acquisition and pre-processing of the images. Figure 3C shows the results of the process in which contrast adjustment was applied in order to increase the background contrast with respect to the spermatozoa.

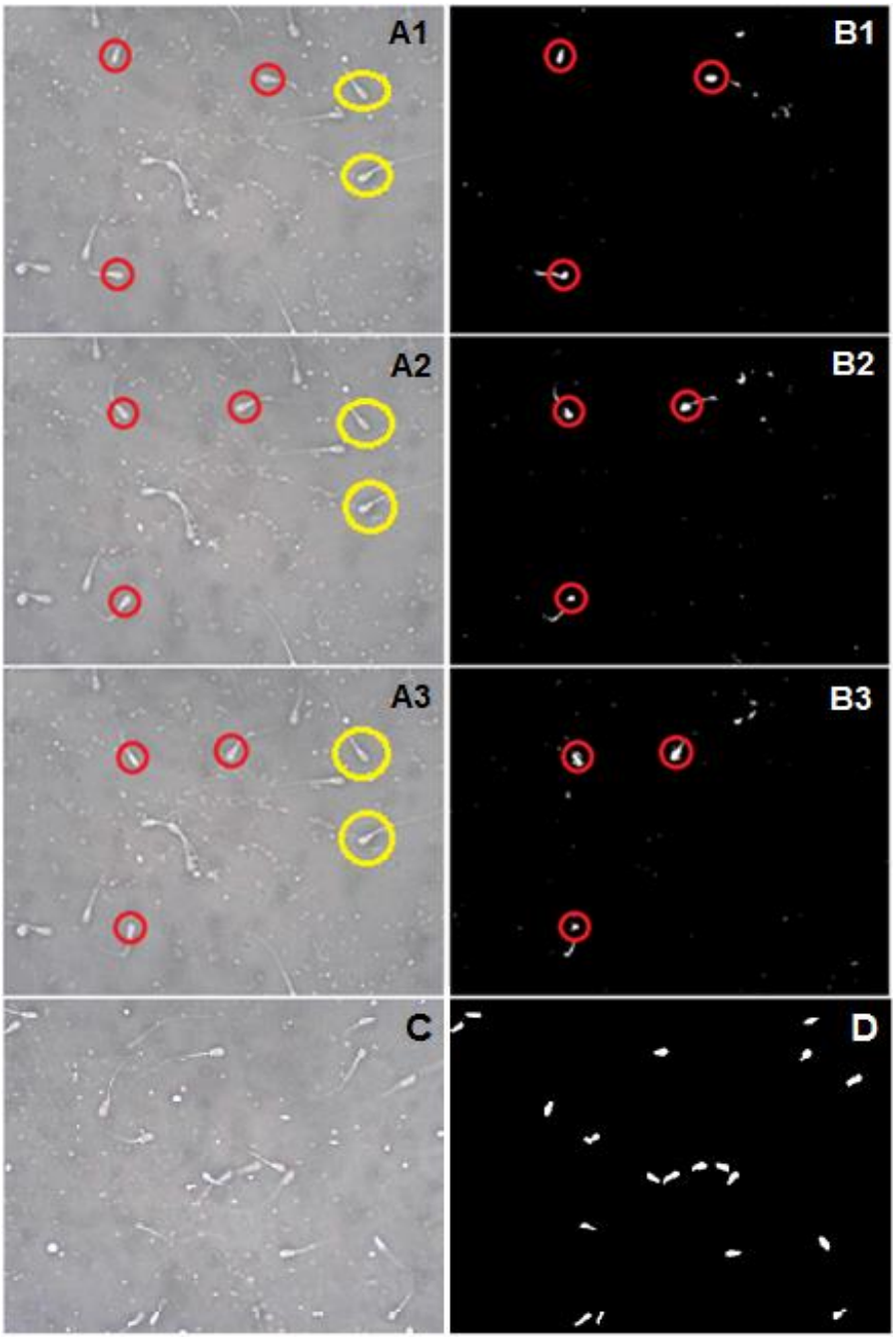

Figure 3. (A1-A3) Sequence of original frames. **(B1-B3)** Sequence of frames showing segmentation of three spermatozoids in motion by the adaptive method of Gaussian models. **(C)** Original frame. **(D)** Fisher discriminant analysis segmentation.

Segmentation and detection of spermatozoids

Segmentation by a combination of adaptive Gaussian models had effect shown in Figures 3B1 to B3. It is evident that these spermatozoids with displacement highlighted by red circles are extracted from the background together with some particles generated by the vibration of the sperm liquid, caused by the turbulence proper to the flagellar movement of spermatozoa. Some sperm tails are also extracted, either completely or partially; also, these spermatozoa have very poor or near zero displacement. Figures 3A1 to A3 highlights spermatozoids in yellow, do not exhibit movement at all and are not segmented by this technique, as expected, because the pixels that constitute them do not show variability or displacement in the video and are practically

taken as part of the background.

Later, the application of morphological operators to the binary image resulting from the segmentation method allowed eliminating the small particles generated by the movement of the background. Also, the tails of the spermatozoa are reduced until they disappear, thus leaving only the heads of the spermatozoids in motion. However, the filtering process is not enough and sometimes it allows the presence of other objects of larger size in the images that do not belong to spermatic heads. For this reason, an aperture operator was applied followed by a closure operator with a circular structuring object of 2- and 4-pixel radius, respectively, in order to obtain an image with objects that belong to the heads of the spermatozoids without disturbances.

Since the adaptive Gaussian models did not segment the sperm without motility, another method was required. For this, Fisher's linear discriminant analysis was used, which allowed the sperm cell heads to be segmented independently of their mobility or vitality, in order to analyze all spermatozoa in the video.

Figure 3C shows the final frame of a test video in which this analysis was done. The corresponding result is shown in Figure 3D, where it is shown that the sperm heads are extracted from the background effectively. Fisher's method segments all sperm heads independently of their movement, since it is based only on their color composition, allowing the detection of these spermatozoa without any movement.

Assignment and construction of trajectories

In Figure 4, the effect of application of the Kalman filter and Munkres algorithm is illustrated. In Figure 4A1 to A3 the transition of three frames at different times is observed, showing the positions of all the detected centroids, labeled with red points. Whereas, in Figure 4B1 to B3, the assignment of these positions to the actual trajectories of the spermatozoids is shown with blue lines.

Likewise, the superposition of two sperm trajectories is shown in Figure 4A3 and B3. However, the Munkres assignment allows proper differentiation of these two trajectories. It was also observed that when the current position of the spermatozoon was not detected, either due to segmentation errors, the Kalman filter enabled the prediction of the position in each frame; therefore, when the target is detected again, the correction of the position should be done to compute the prediction model with the current measurement.

Characterization of sperm motility

With the Kalman filter, it was possible to define the trajectory of each moving sperm present in the video. A trajectory is described as a series of Cartesian coordinates in the image; this allows characterization and classification of each spermatozoon within a degree of motility just like the commercial CASA systems. Figure 4C shows the final frame of the trajectory as described in Figure 4A3, where it is observed that for each trajectory, the VCL, VAP and VSL are calculated to proceed to the classification stage.

Finally, in Figure 4D, the expansion of a trajectory was performed to show the classification process. In this case, a very undulating movement of a spermatozoid (WOB = 47.3%) combined with a very low linearity (LIN = 39.1%) was observed, which makes it a spermatozoon without progressivity belonging to category C.

Validation of the computational tool

The evaluation performed by the andrology expert was based on the same classification criteria described in the state of the art except for categories A and B. Categories A and B are linked in a single class (A + B) for practical effects, because, according to the expert, it is often unnecessary to distinguish between fast and low progressive spermatozoa. Taking this into account, the classification is as follows:

1. Class 1: spermatozoa with progressive motility (Category A + B);
2. Class 2: spermatozoa with non-progressive motility (Category C);
3. Class 3: sperm without motility (Category D).

From these classes, the calculation of the total sperm detected (total), percentage of progressive motility (% MP) and percentage of total motility (% MT) were derived. Thus, the observation and assessment obtained from the 10 videos by the andrology expert are shown in Table 1. It shows the number of sperm classified in each category and percentages of progressive and total motility.

On the other hand, the analysis of the 10 videos of seminal samples from different bulls was arranged and the algorithm was executed to show results in terms of the parameters of motility observed by the expert. Table 2 shows the results obtained by the computational tool.

Likewise, the determination coefficients were calculated in order to find the level of success of the computational tool developed with respect to the analysis performed by the expert. Figure 5A shows the correlation of spermatozoa in the (A + B) category for the expert and the algorithm. It is shown that the computational tool was able to classify most progressive spermatozoa with a high determination coefficient (R2 = 0.8542).

However, there were differences in the detection and classification of spermatozoa belonging to category C. Figure 5B shows that the correlation was low with a coefficient of determination of R2 = 0.3952. This was

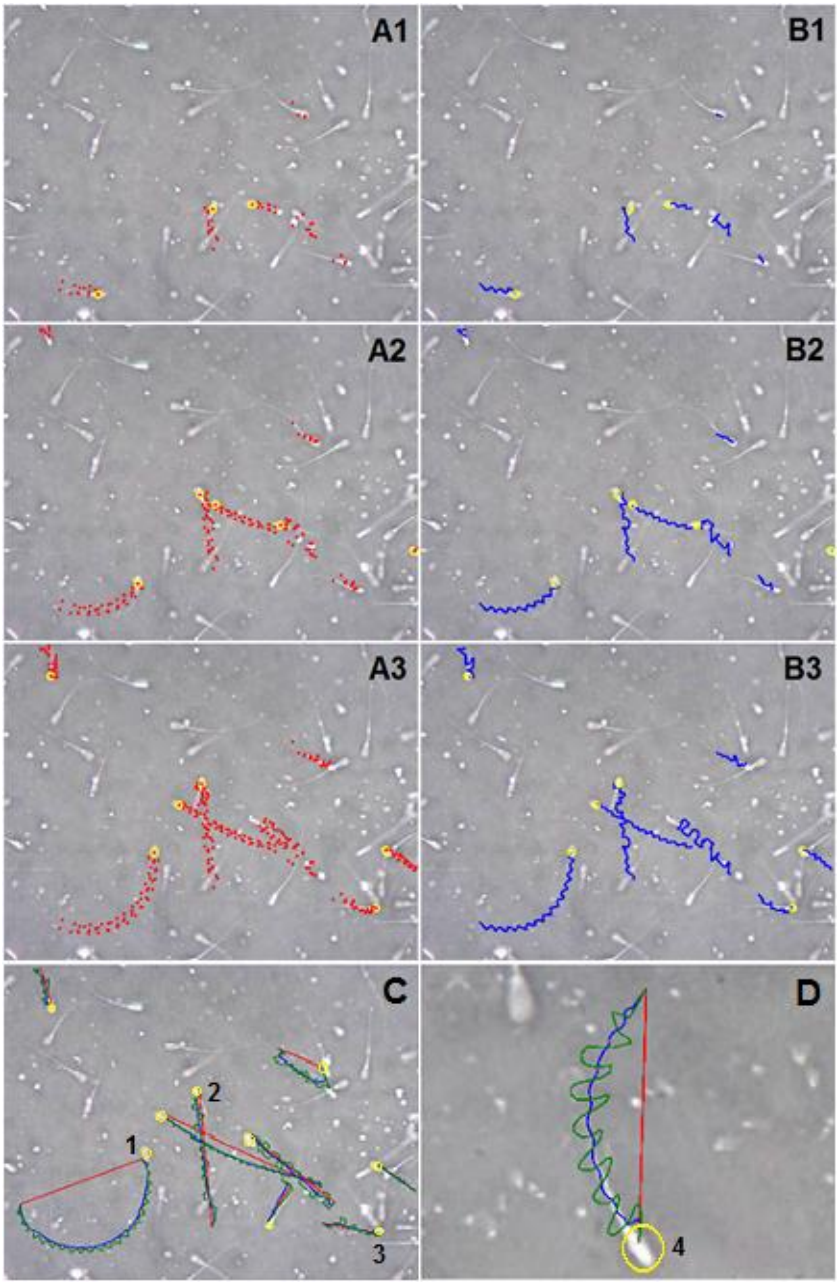

Figure 4. Frames at different times: 1, 2, 3. (A) in red dots, unassigned centroid detections are marked; (B) in blue lines, the constructed trajectories are illustrated; (C) trajectories are characterized; VLC in green; VAP in blue; VSL in red; (D) characterized trajectory of a random spermatozoon.

mainly due to the difficulty in adjusting a minimum sensitivity threshold in order to sort a moving and non-progressive sperm, because the visual inspection of the expert is very subjective and there is no strict regimen, for example, when considering a spermatozoon with almost null displacement or with extremely short displacement. On the other hand, for the detection of non-motile spermatozoa, a good correlation (R2=0.8056) was observed, therefore, Fisher's discriminant analysis had a good performance, as shown in Figure 5C.

In general terms, it can be stated that the motile classification stage of the algorithm presented good agreement with the expert's manual analysis, since by combining the data of the three classes, a percentage of progressive motility of R2 = 0.8143 and high correlation with a coefficient of determination of R2 = 0.8754 can be

Table 1. Results of manual analysis by the expert technician, elaborated by the author.

Video	Cat. A+B	Cat. C	Cat. D	Total	MP (%)	MT (%)
1	7	2	19	28	25.00	32.14
2	6	1	13	20	30.00	35.00
3	3	1	10	14	21.43	28.57
4	2	2	3	7	28.57	57.14
5	5	0	4	9	55.56	55.56
6	7	1	9	17	41.18	47.06
7	2	3	7	12	16.67	41.67
8	5	2	5	12	41.67	58.33
9	5	0	9	14	35.71	35.71
10	6	1	11	18	33.33	38.89

Table 2. Results obtained with the computational tool, elaborated by the author.

Video	Cat. A+B	Cat. C	Cat. D	Total	MP (%)	MT (%)
1	7	1	19	27	25.93	29.63
2	6	0	13	19	31.58	31.58
3	2	2	9	13	15.38	30.77
4	3	0	4	7	42.86	42.86
5	5	1	2	8	62.50	75.00
6	8	2	7	17	47.06	58.82
7	3	0	12	15	20.00	20.00
8	4	0	7	11	36.36	36.36
9	5	2	7	14	35.71	50.00
10	6	1	11	18	33.33	38.89

obtained as shown in Figure 5D and E, respectively.

Finally, using the Bland-Altman test shown in Figure 5F, which represents the difference between the methodologies implemented, no significant variability was found between the sperm motility measurement by the expert and the implemented computational tool. The outcomes show the differences of the manual measure with respect to the algorithm with a relation of 0.966 in a 95% confidence interval of (3.058 to 3.19). They indicated that the measurements were very similar, if the two methodologies were the same, the expected ratio would be 1.

DISCUSSION

In the present work, the versatility of the artificial vision is demonstrated in processes that require observation of small objects on microscopic images for long periods of time. This application provides a technological support to the manual analysis by the expert, and in this way, the intrinsic drawbacks of his intervention are greatly reduced. However, it is necessary to use an expert to properly focus the sample of the ejaculate and obtain videos of high quality.

It is important to note that the present methodology aimed only at post-thawed samples and fresh ejaculates were not supported. Though fresh spermatozoa have similar performance than the frozen counterpart (Szeptycki and Bentov, 2016), their captures under microscope and kinetics are different.

The preparation of the semen samples was carried out according to the protocols established in the World Health Organization (WHO, 2010) laboratory manual, in order to remove agglomerations of cells that could impair the procedure. Moreover, the image capture was obtained using a suitable illumination and focus configuration of a binocular microscope Leica model DM500 led, with digital camera, Wi-Fi model ICC50W. Each capture was taken immediately after thawing because sperm vitality decreases over time (Ibânescu et al., 2016).

Disadvantages were evidenced in some samples due to the cases in which some spermatozoa were defocused by the change of their height within the sample, which caused erroneous detections in the segmentation. The contrast adjustment allowed this situation to be improved by facilitating the method to recognize variation in pixel

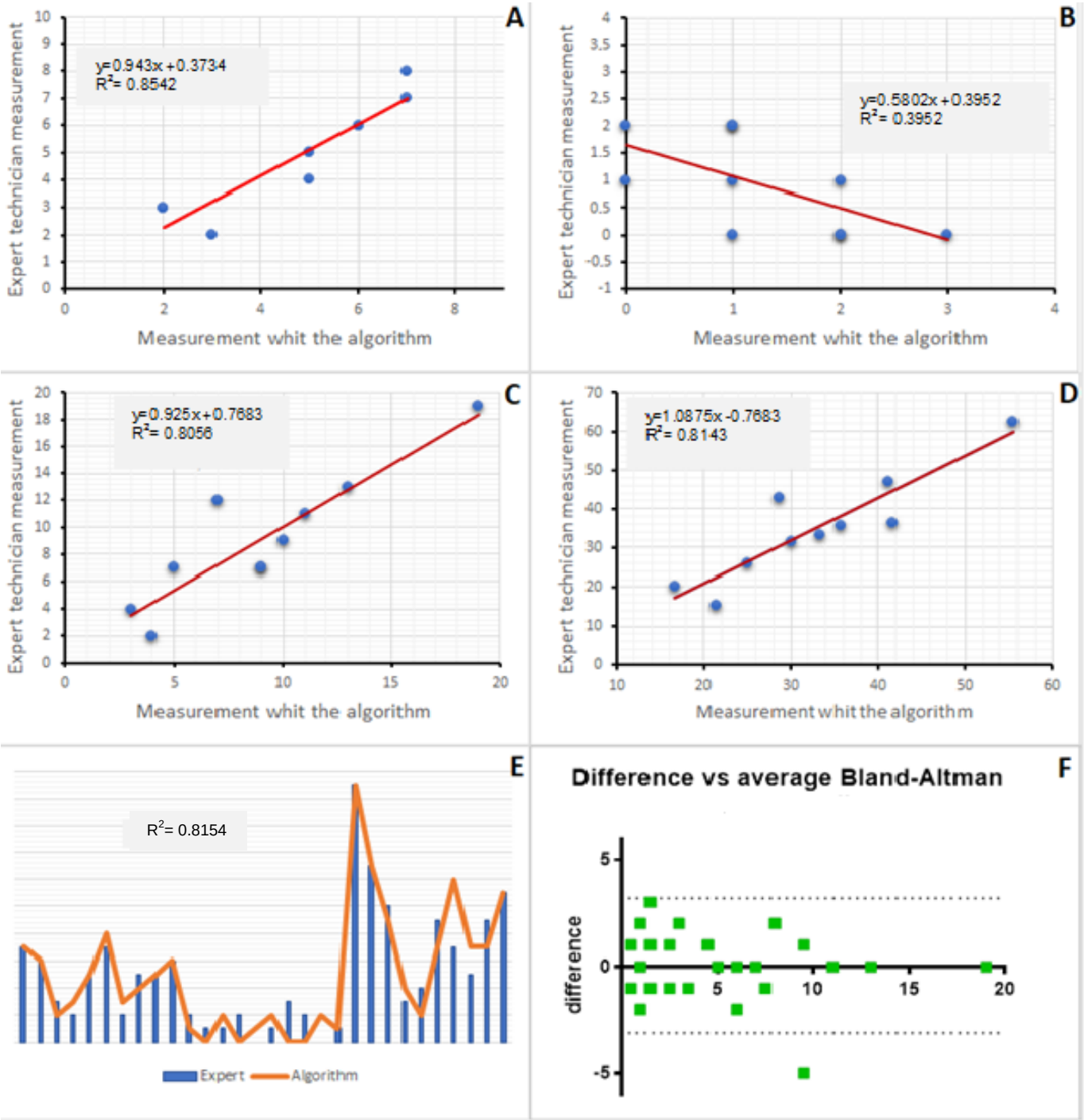

Figure 5. (A) Linear regression and coefficient of determination of spermatozoa classified in A + B, (B) Linear regression and coefficient of determination of spermatozoa classified in C, (C) Linear regression and coefficient of determination of spermatozoa classified in D, (D) Linear regression and coefficient of determination of the percentage of progressive motility calculation, (E) Correlation between the computational tool vs. the expert technician, (F) Bland-Altman test for classes A+B, C and D.

values along the frames.

Due to the vibration of the seminal fluid caused by the oscillatory movement of the sperm tails, there was an exaggerated detection of particles not corresponding to sperm heads; therefore, morphological operators were implemented to eliminate them in the field of the binary image. This could be avoided if a non-linear diffusion filter is used as shown by Imani et al. (2014), but morphological

operators were enough. In this way, only the regions belonging to the spermatic heads were obtained, which through an analysis of connected components were extracted from the values of the position coordinates in each frame.

The adaptive mixture of Gaussian models algorithm is one of the useful techniques for background subtraction as summarized by Piccardi (2004). It allowed a proper detection of movement in the cells that presented displacements, but those immobile ones were not segmented. Therefore, a Fisher´s linear discriminant analysis was implemented to extract all the sperm cells using an experimentally extracted database to perform a complete motility analysis. Fisher method offers great precision of segmentation, but consumes a high amount of memory and processor (Zhiwei et al., 2012); thus, for higher resolutions, it could take significant periods of time.

Furthermore, the criterion of eccentricity made it possible to discard non-spermatozoa objects in the segmentation process, making the method more reliable. However, in certain specific cases, segmentation errors were observed, where two sperm heads that are in contact were taken as a single object and were therefore ignored by the area criterion. Watershed algorithms and particle filters were able to break this contact in the segmentation process (Ravanfar et al., 2014).

The reconstruction of each sperm trajectory in the video was possible due to the implementation of the Munkres assignment algorithm; it could assign the new centroids to the existing trajectories using the Kalman filter prediction and correction criteria. This filter, whose initial variables were adjusted experimentally, worked correctly in the individual tracking process. A common issue found in multi-tracking algorithms is the problem derived from the superposition of targets. Since each sperm trajectory develops its own Kalman filter, this issue was solved (Urbano et al., 2017).

Despite not having an official protocol for the CASA systems, one was adapted for the present design, by characterizing the coordinates that describe the trajectory of each motile spermatozoon in the video. This allowed calculation of the parameters of individual motility according to the commercial systems CASA. Starting from the acquisition of these parameters and the classification of motility, for each video, a percentage of progressive motility was obtained, which was submitted to validation having as reference, the assessment by an expert in andrology.

The validation regarding observation and manual analysis by a technician showed high concordance in the classification of progressive motility. However, the classification of non-progressive motility was affected, mainly by the complexity of the objective determination of the speed limits or cut-off values of non-progressive and almost immotile spermatozoa (Wilson-Leedy and Ingermann, 2007), because the sensitivity of the algorithm is quite different as compared to the human eye and the conventional manual procedure presents downsides (Baracaldo et al., 2007). This could be overcome but it would require higher frames per second.

This affected the total motility analysis, but the results showed that they followed the trend line of the data provided by the expert. On the other hand, the parameter of progressive motility, one of the significant descriptors for fertility together with VAP and VSL (Ahmed et al., 2016) (Rezagholizadeh et al., 2015), had a high coefficient of determination (R2=0.8143) and, therefore, a very good correlation.

As also demonstrated by Giaretta et al. (2017), open alternatives are as competitive as commercial systems like Hamilton-Thorne IVOS and present similar performance for sperm motility analysis, even though there is no official standard for computer-assisted tools.

Thus, a semi-automatic, reconfigurable and modular computational tool was developed for the assisted analysis of individual sperm motility of bovine semen samples. It has the capacity to reduce human errors in the interpretation of motility parameter and thus provide reliable results. In Colombia, this tool would provide an economical and accessible alternative for quality analysis, academy and research in the field of andrology and veterinary medicine.

Future developments involve, firstly, the minimization of errors presented in this study, then, the design of a complete CASA system with the capacity to analyze motility and viability, concentration and sperm morphology. In addition, adjusting the design to provide the user with the option of evaluating both bovine semen samples and other animal species, is proposed.

CONFLICT OF INTERESTS

The authors declare that there is no conflict of interest.

ACKNOWLEDGEMENTS

The authors thank the expert staff of the andrology laboratory of Universidad Nacional de Colombia for the support in the acquisition of videos and assistance in the detection of sperm parameters. They also thank Walter Cardona-Maya of Universidad de Antioquia for his valuable assistance in manual analysis of sperm motility, which enabled the validation of the proposed system.

REFERENCES

Agarwal A, Sharma RK (2007). Automation is the key to standardized semen analysis using the automated SQA-V sperm quality analyzer. Fertil. Steril. 87(1):152-162.

Ahmed H, Hassan Andrabi S, Jahan S (2016). Semen quality parameters as fertility predictors of water buffalo bull spermatozoa during low-breeding season. Theriogenology 86(6):1516-1522.

Baracaldo M, Barth A, Bertrand W (2007). Steps for Freezing Bovine Semen: From Semen Collection to the Liquid Nitrogen Tank. IVIS

Reviews in Veterinary Medicine. Available from: http://www.uesc.br/cursos/pos_graduacao/mestrado/animal/bibliografia2007/baracaldo_et_at_2007.pdf.
Bishop C (2006). Pattern recognition and machine learning. Springer, Cap 4:179-220.
Contri A, Valorz C, Faustini M, Wegher L, Carluccio A (2010). Effect of semen preparation on casa motility results in cryopreserved bull spermatozoa. Theriogenology 74(3):424-435.
DANE (2016). Monthly bulletin, inputs and factors associated with agricultural production. Livestock cattle for the production of meat in Colombia, under good livestock practices. https://www.dane.gov.co/files/investigaciones/agropecuario/sipsa/Bol_Insumos_feb_2016.pdf.
Giaretta E, Munerato M, Yeste M, Galeati G, Spinaci M, Tamanini C, Mari G, Bucci D (2017). Implementing an open-access CASA software for the assessment of stallion sperm motility: Relationship with other sperm quality parameters. Anim. Reprod. Sci. 176(1):11-19.
Gonzalez R, Woods R (2008). Some basic relationships between pixels: Digital Image Processing. Prentice Hall., Cap. 2:34-71.
Hidalgo O, Tamargo M, Diez M (2017). Análisis del semen bovino. http://www.serida.org/pdfs/1495.pdf.
Ibânescu I, Leiding C, Gregore S, Rosca P, Sfartz I, Drugociu D (2016). Differences in CASA output according to the chamber type when analyzing frozen-thawed bull sperm. Anim. Reprod. Sci. 166:72-79.
Imani Y, Teyfouri N, Reza M, Golabbakhsh M (2014). A New Method for Multiple Sperm Cells Tracking. J. Med. Signals Sensors 4:35-42.
Kalman R (1960). A new apprach to linear filtering and prediction problems. J. Basic Eng. 82:35-45.
Livestock Context (2017). Bull semen, key to milk production with more protein and fat. http://www.contextoganadero.com/internacional/semen-de-toro-clave-en-produccion-de-leche-con-mas-proteina-y-grasa.
Lu JC, Huang YF, Lu NQ (2014). Computer aided sperm analysis: past. Present and future. Andrology 46(4):329-338.
Maintz T (2005). Mathematical morphology. Digital and medical image processing. Cap 6:121-160.
Munkres J (1957). Algorithms for the assignment and tranportation problems. J. Soc. Ind. Appl. Math. 5:32-38.
Nagy Á, Polichronopoulos T, Gáspárdy A, Solti L, Cseh S (2015). Correlation between bull fertility and sperm cell velocity parameters generated by computer-assisted semen analysis. Acta Vet. Hung. 63(3):370-381.
Piccardi M (2004). Background subtraction techniques: a review. IEEE International Conference on Systems, Man and Cybernetics. DOI 10.1109/ICSMC.2004.1400815. Available from: http://ieeexplore.ieee.org/document/1400815/.
Ravanfar M, Azinfar L, Hassan Moradi M, Fazel-Rezai R (2014). Occlusion Robust Low-Contrast Sperm Tracking Using Switchable Weight Particle Filtering. Adv. Sex. Med. 4:42-54.
Rezagholizadeh A, Gharagozlou F, Niasari-Naslaji A, Akbarinejad V, Ziapour S (2015). Evaluation of Sperm Characteristics in Caspian Stallions Using Computer-Assisted Sperm Analysis. J. Equine Vet. Sci. 35:505-509.
Simonik O, Šichtař J, Stádník L, Biniova Z (2015). Computer assisted sperm analysis – The relationship to bull field fertility, possible errors and their impact on outputs: A review. Indian J. Anim. Sci. 85:3-11.
Stauffer C, Grimson W (1999). Adaptive background mixture models for real-time tracking. http://citeseerx.ist.psu.edu/viewdoc/download?doi=10.1.1.88.877&rep=rep1&type=pdf.
Szeptycki J, Bentov Y (2016). Cryopreservation of Embryos and Gametes: Past, Present, and Future. Cryopreservation in Eukaryotes. Available from: https://www.intechopen.com/books/cryopreservation-in-eukaryotes/cryopreservation-of-embryos-and-gametes-past-present-and-future.
Urbano L, Masson P, VerMilyea M, Kam M (2017). Automatic Tracking and Motility Analysis of Human Sperm in Time-Lapse Images. IEEE Trans. Med. Imaging 36(3):792-801.
Vincent P, Underwood S, Dolbec C, Bouchard N, Kroetsch T, Blondin P (2012). Bovine semen quality control in artificial insemination centers. Anim Reprod. 9(3):153-165.
Wilson-Leedy J, Ingermann R (2007). Development of a novel CASA system based on open source software for characterization of zebrafish sperm motility parameters. Theriogenology 67(3):661-672.
WHO-World Health Organization (2010). Laboratory manual for the Examination and processing of human semen. 5th Ed. Switzerland.
Ye Z, Hu Z, Lai X, Chen H (2012). Image Segmentation Using Thresholding and Swarm Intelligence. J. Softw. 7(5):1074-1082.

African Journal of Biotechnology

Related Journals Published by Academic Journals

- *Biotechnology and Molecular Biology Reviews*
- *African Journal of Microbiology Research*
- *African Journal of Biochemistry Research*
- *African Journal of Environmental Science and Technology*
- *African Journal of Food Science*
- *African Journal of Plant Science*
- *Journal of Bioinformatics and Sequence Analysis*
- *International Journal of Biodiversity and Conservation*

academicJournals